CHARACTERIZATION OF GAS-LIQUID-LIQUID TUBULAR REACTORS

BY

Savvas G. Hatzikiriakos

A Thesis submitted in conformity with

the requirements for the Degree of

MASTER OF APPLIED SCIENCE

at the

Department of Chemical Engineering and Applied Chemistry

UNIVERSITY OF TORONTO

Under the direction of

Professor J.M. Shaw

1988

To

Georgios and Stavroula

who took considerable pain

to raise and educate me.

Acknowledgements

I would like to express my sincere appreciation to Prof. J.M. Shaw for his skillful guidance, friendship and financial support.

Sincere thanks to Dr. R.P. Gaikwad for his assistance in the experimental section and in the image analysis part of this investigation.

Special thanks to Prof. S. Rizvi for his personal interest in this research and for his counselling on how to be both a good human being and an incisive scientist.

Deep gratitude is due to Stella and Tolis Karasavvas for their spiritual and moral support in the absence of my parents.

Finally, undying love to Christina without whose long distance company in the lonely nights during the final phase of this work, it would have not attained the desired height.

ABSTRACT

In this investigation, the impact of gas flux and physical properties of dispersed phase constituents on unsteady and steady-state drop size distributions of dispersed phase drops in gas-liquid-liquid tubular reactors is quantified. Experiments were performed with three model ternary dispersed phase systems including linseed oil+trichloroethylene-water -air, cottonseed oil+ trichloroethylene-water-air and dibenzyl ether-water-air. The relative importance of dispersed phase viscosity, interfacial tension and the density difference between the two liquid phases are assesed independently. The physical properties of the dispersed phase are shown to have a significant impact on the steady-state mean drop size and drop size distribution at low gas fluxes. However, at high gas fluxes, the effect of dispersed phase physical properties is less significant. A new theory is proposed to explain the functional dependence of the maximum and minimum drop sizes, stable against break-up and coalescence, on the energy dissipation rate. Gas flux and physical properties of the dispersed phase constituents were not found to have a significant effect on the rate at which steady-state is reached. The existence of a similarity variable which is very helpful in estimating the drop size distribution as a function of time is identified. Mean drop size and drop size distributions are correlated using theoretical models for drop break-up and coalescence in turbulent flow fields and these results are compared with stirred tank analogues.

TABLE OF CONTENTS

APPENDICES

LIST OF TABLES

LIST OF FIGURES

1.0 INTRODUCTION

The dispersion of one phase in another phase in multiphase systems is of great importance in chemical engineering, specifically for processes involving heat and mass transfer. Moreover, hydrodynamic effects arising in these systems play an important role in determining the kinetic schemes and rates of transport processes associated with these systems. The design of multiphase reactors requires the study of both hydrodynamic effects and phase interactions. Studies related to two-phase systems are numerous. However, phase interactions associated with gas-liquid-liquid systems have received comparatively little attention even though these systems arise frequently in chemical engineering applications. For example, the reaction environment and kinetic schemes associated with the direct hydrogenation of bitumen and coal liquids are complex. Apart from vapour and solid phases, two liquid phases may also co-exist. Recently, Shaw et.al. (1988) carried out experiments using a model coal liquefaction solvent (pyrene-tetralin) and showed that two liquid phases can arise under coal liquefaction conditions. The transfer of hydrogen from the gas phase to the dispersed liquid phase has been identified as a potential rate limiting phenomenon in coal liquefaction. As the mass transfer rate limitation occurs at the liquid-liquid interface, mean drop size distribution becomes a key variable. In addition, the hydrogen bubbles may impose turbulent flow conditions while passing through the reactor. The criteria for bubble/drop

stability in isotropically turbulent two phase flow have been defined statistically by Thomas (1981). Such conditions are sufficiently intense to cause drop splitting and the generation of large interfacial areas, depending on the availability of hydrogen.

Phase interactions arising in these systems have been investigated in the present work using various physical models. The impact of gas-bubble liquid-drop interaction on the steady-state liquid-liquid interfacial area is emphasized. Moreover, the simultaneity of drop breakage and transport processes (heat and mass transfer) brings about the need for knowledge of drop size and drop size distribution as a function of time.

Due to the complexity of gas-liquid-liquid systems several characteristics related to these systems have been assessed and discussed independently. Bubble generation and motion are among the most important parameters influencing the operation of the phase-contacting equipment. As the bubbles move upwards, turbulent conditions are imposed throughout the reactor. Bubbles with different sizes have different terminal velocities and impose turbulent conditions with various levels of intensity. The rate of the energy dissipation is related to the intensity of turbulence and controls drop splitting. It also has a severe impact on the generation of interfacial area. Physical properties of the liquids are also expected to have a significant impact on the steady-state drop size and drop size distribution. The impact of various physical properties including

interfacial tension, viscosity and density is discussed. The behavior of gas-liquid-liquid systems in tubular reactors may be compared with liquid-liquid systems in agitated vessels by considering the respective roles of the gas-phase and the impeller in these reactor types. Thus, characteristics related to liquid-liquid systems in agitated vessels may provide some understanding of the behavior of gas-liquid-liquid systems in tubular reactors.

The various characteristics mentioned above are summarized in a generalized correlation for evaluating the steady state interfacial area in gas -liquid-liquid tubular reactors. It should be noted that the proposed correlation includes a broad range of operating conditions and dispersed phase properties. Also an attempt is made to model transient drop break-up so that the transient interfacial area can be known as a function of time. A new theory is proposed which is intended to elucidate the phase interactions related to gas-liquid-liquid systems in tubular reactors.

These various aspects may be used in establishing criteria for the design of G-L-L tubular reactors. It also improves the reactor operation and process control strategies. Once design criteria have been established, the following improvements over the existing tubular reactors are expected:

-a narrower residence time distribution for the dispersed phase

-improved gas-liquid mass transfer rates

-a reduced gas flux requirement

So far, the mechanism of drop splitting and the implications for the design and operation of industrial gas-liquid-liquid tubular reactors are unresolved even if they arise in chemical engineering applications. The present work sheds light on phase interactions arising in gas-liquid-liquid tubular reactors and proposes the further investigation which has to be done until these reactors might be applied efficiently in industry.

PART I

THEORETICAL

2.0 LITERATURE REVIEW

Phase interactions in gas-liquid, gas-solid, liquid-liquid and gas-liquid-solid systems have been the subjects of numerous experimental and theoretical investigations (Kumar et.al.,1976; Kito et.al.,1976; Begovich and Watson,1978; Hikita et.al., 1980; Kato et al.,1982; Stamatoudis and Tavlarides, 1985). However, phase interactions arising in gas-liquid-liquid systems have received comparatively little attention, even though such three phase systems can arise in hydrorefining processes (Shaw et.al.,1988), pyrometallurgical processes (Guthrie and Bradshaw 1969) and electroorganic synthesis. Yoshida and Yamada (1972) first measured the average diameter of kerosene drops dispersed in bubble columns which were operated in batch mode with respect to both continuous and dispersed phase liquids. The Sauter mean diameter was correlated as a function of power consumption per unit mass of liquid and volume fraction of dispersed phase liquid. The mean drop size was found to be roughly proportional to the power input (power input$^{-0.5}$) and to the volume fraction of the dispersed liquid phase (volume fraction$^{0.25}$). They also found that tubular reactors are more efficient contactors than agitated reactors for liquid-liquid systems as far as mean drop size is concerned. However, they did not consider the effect of physical properties of the dispersed and continuous phases. An empirical correlation relating mean drop size to column diameter and dispersed phase viscosity was

subsequently proposed by Hatate (1976).

Recently, Kato et al. (1984) carried out experiments in a multistage bubble column to simulate gas-liquid-liquid systems. The Sauter mean drop diameter was correlated as a function of superficial gas velocity, liquid velocity and free area of horizontal baffle plates. The operation of their column was continuous with respect to all three phases. However, it was unclear whether or not steady state was reached as far as mean drop size is concerned.

The behavior of gas-liquid-liquid systems is poorly characterized in the open literature. To gain a better understanding of the behavior of G-L-L systems, the behavior of gas-liquid systems in tubular reactors and liquid-liquid systems in agitated vessels are reviewed. In addition, bubble formation at orifices and drop break-up in turbulent flow fields may shed light on the controlling mechanisms of drop break-up in G-L-L systems.

2.1. Bubble Formation

Bubble formation is one of great importance in the operation of phase-contacting equipment for gas-liquid, gas-liquid-liquid and gas-liquid-solid systems. A variety of atomizers, spray nozzles and orifices have been devised for bubble generation. Each of these devices has different characteristics which have been reviewed (Kumar and Kuloor, 1970; Lane and Green, 1956; Clift et al., 1978). The various bubble sizes

generated by the above devices play an important role in determining the kinetic schemes and rates of transport processes associated with multi-phase systems (Shaw, 1985). An examination of the various parameters influencing bubble generation will shed light in understanding the operation of such multi-phase systems.

In the present work, bubbles are formed at a multi-nozzle plate located at the bottom of the column. When a bubble is formed at such a nozzle, the pressure within the bubble decreases due to its upward motion. Thus the gas rate may vary with time (Clift et al.,1978). Therefore, we can consider two distinct cases for bubble generation. When there is a relatively high pressure drop between the gas reservoir and the nozzle, the pressure fluctuations due to bubble formation are insignificant. In this case the gas flow can be taken constant and the bubbles are formed under constant flow conditions. The other extreme situation is taken when the chamber volume is very large by comparison with the bubbles being formed. This case, where the bubble generation does not change the pressure in the chamber, corresponds to bubble formation under constant pressure conditions. The intermediate range is called bubble generation under intermediate conditions. The division of bubble formation into three different mechanisms is quite fundamental since it allows for a broad range of bubble volumes at the same gas flow rate. Bubble volumes formed under constant pressure conditions are several times larger than those under

constant flow conditions at the same flow rate (Clift et al.,1978).

Davidson and Schuler (1960) were the first to distinguish these three bubble formation regimes. Tsuge and Hibino (1983) reviewed various correlations of bubble volume and classified the phenomenon of bubble generation into three groups using the dimensionless capacitance group N_c proposed by Hughes et al. (1955).

1. $N_c < 1$ Constant flow conditions
2. $1 < N_c < 9$ Intermediate conditions
3. $N_c > 9$ Constant pressure conditions

where,

$$N_c = 4V_c g\rho_l / \pi D_o^2 P_h$$

and V_c is the volume of the chamber, g the gravitational accelaration constant, ρ_l the density of the liquid, D_o the diameter of the orifice and P_h the hydrostatic pressure at the orifice plate.

Davidson and Schuler (1960) also divided each of the above ranges into three subranges:

1. $N_w < 2.4(N_c-1)$ Uniform bubbles are formed
2. $2.4(N_c-1) < N_w < 16$ The bubble volume increases with the increase of N_w.

3. $N_w > 16$ The bubbles break down after detachment at the orifice.

where,

$$N_w = BoFr^{0.5}$$

and Bo, Fr are the dimensionless Bond and Froud numbers respectively.

There are many theoretical and experimental studies concerning bubble formation at orifices (Kumar and Kuloor, 1970; Davidson and Schuler, 1960; Marmur and Rubin, 1973; Lanauze and Harris, 1973; Wraith, 1971; Marmur and Rubin, 1976; McCann and Prince, 1969). Davidson and Schuler (1960) have derived simple expressions for bubble volume under constant flow conditions in viscid and inviscid liquids. These equations are functions of gas rate and viscosity of continuous phase. The contradiction in the existing data, regarding the role of viscosity in bubble formation has been discussed by Kumar and Kuloor (1970). Generally the effect of viscosity is large at high gas flow rates (Kumar and Koolor, 1970; Ruff, 1972; Wraith, 1971; Ramakrishnan, 1969) and bubble volume increases with viscosity of continuous phase. The same trend has been found for the case of constant pressure conditions (Kumar and Kuloor, 1970; Davidson and Schuler, 1960; Satyanarayan et al., 1969). Gas flow rate controls the mechanism of bubble formation. At low gas flow rates, separate bubbles are formed (Schugerl et al.,1977). At intermediate gas flow rates, bubble size is controlled by the instability of the jet interface (Meister and Scheele,1967). At high gas

flow rates bubble size is controlled by interfacial forces and dynamic pressure forces of the local turbulence (Hinze,1955).

Interfacial tension affects bubble volume at low flow rates and has a negligible effect at high flow rates (Kumar and Kuloor,1970). However, a more detailed analysis takes into consideration the effect of continuous phase viscosity and interfacial tension (Satyanarayan,1969). Another significant factor influencing bubble volume is the orifice diameter. At low gas rates, the effect of orifice size is such that the volume of the bubble increases with orifice size. At higher flow rates bubble volumes for various orifice diameters tend to join in a single curve (Kumar and Kuloor,1970; Ramakrishnan,1969).

Other parameters affecting bubble generation include: orifice characteristics, chamber volume, submergence, liquid density, gas physical properties, gas flow rate and continuous phase viscosity. Reported data are inconsistent and reflect a lack of appreciation by various investigators for the effects of chamber volume, the types of flows and the interactions of several variables considered (Clift et al.,1978). Because of these contradictions in the reported data bubble sizes are measured directly in the present work using a photographic technique.

2.2. Terminal Velocities of Bubbles

Bubbles/drops rise or fall freely in infinite media under the influence of

various forces e.g. gravitational, inertial, buoyancy and drag forces (Clift et al.,1978). Shape is controlled by the drag force which in turn determines the terminal velocity. For Reynolds numbers less than unity the inertia forces are negligible in comparison with viscous and interfacial tension forces. In this case, bubbles or drops are closely approximated by spheres. The terminal velocity and drag coefficient have been found analytically by Hadamard (1911) and Rybczynski (1911) who indepedently solved the Navier-Stokes equations. At high Reynolds numbers, spherical bubbles and drops are deformed to an ellipsoidal shape. In this case surface tension, contaminants and secondary motion imposed by the internal circulation of fluid particle play an important role in determining terminal velocities. Surface contaminants are inevitable and for many practical purposes one has to consider them. Grace et al. (1976) has correlated a substantial amount of data reported in the literature. Bubble/drop deformation is more pronounced as the Reynolds number is increased further. For Re>150, the rear is quite flat and the wake angle θ_w is given (Clift et al.1978) by,

$$\theta_w = 50^o + 190\exp(-0.62Re^{0.4})$$

Davies and Taylor (1950) have derived a simple expression for the terminal velocity of spherical-cap fluid particles for relatively high Reynolds numbers. Their calculations were based on equating the pressure distribution around the particle (potential flow) and the pressure distribution on the surface of the particle (hydrostatic pressure). Their

correlation is as follows:

$$U_T=(2/3)[g\alpha(\rho_l-\rho_g)/\rho_l]^{1/2} \qquad \text{for} \quad 40 < Re < 150 \qquad (2.1)$$

Where U_T is the terminal velocity of bubble and α the equivalent radius of the bubble. For Reynolds numbers greater than 150 and spherical- cap fluid particles the terminal velocity can be calculated from the following correlation (Clift et al. 1978) which is similar to the Davies and Taylor equation.

$$U_T=0.711[gd_e(\rho_l-\rho_g)/\rho_l]^{1/2} \qquad \text{for} \quad Re>150 \qquad (2.2)$$

Where d_e is the equivalent bubble diameter. This correlation was derived from the geometrical similarity of a spherical- cap fluid particle with a wake angle of approximately 50^0, once Re is greater than about 150.

All the above equations are valid for individual bubbles. In a laminar flow field, bubbles interact and the above equations cannot be applied to estimate bubble swarm velocities. However, Ueyama and Miyauchi (1979) calculated bubble swarm velocities in a turbulent flow field using the above expressions with the Sauter mean diameter d_{vs} instead of d_e and found good agreement with experimental data. Thus, in a turbulent flow field the bubbles have limited interactions. Each bubble rises indepedently. Therefore, the slip velocity of a bubble swarm can be defined as:

$$u_s=0.711[gd_{vs}(\rho_l-\rho_g)/\rho_l]^{1/2} \qquad \text{for} \quad Re > 1000 \qquad (2.3)$$

The bubble swarm velocity can easily be related to the superficial gas

velocity u_g through a simple expression, which is discussed in the next section.

2.3. Gas-Liquid Systems

Gas-liquid bubble column reactors are used extensively in chemical industries because of their various advantages i.e., low investment cost, low energy requirements and effective mixing. Examples include slurry-phase hydrogenation, aerobic biochemical reaction and polymerization of olefins. In this section some of the hydrodynamic parameters associated with gas liquid systems are discussed. Gas holdup is one of the most important hydrodynamic parameters characterizing such systems. It has two applications. On the one hand, it gives the volume fraction of gas in multi-phase systems. On the other hand, the gas holdup in combination with the mean bubble diameter allows the estimation of interfacial area. The existing correlations for gas holdup in the literature are functions of superficial gas velocity, column diameter, orifice size and physical properties of continuous phase (Hughmark,1967; Akita and Yoshida,1973; Kumar et al.,1976; Hikita et al.,1980; Shah et al.,1982). Gas holdup can be calculated directly from bed expansion as,

$$\varepsilon_g=(H-H_o)/H_o \qquad (2.4)$$

where ε_g is the gas holdup, H_o the initial height of liquid in the column in cm

and H is the head pressure in cm of liquid in the column, or indirectly by the manometric method:

$$\varepsilon_g = dP/dh \qquad (2.5)$$

Where dP is the differential pressure drop over a differential height dh of the column. The reported data related to gas holdup promote a scatter due to the sensitivity of the holdup to the gas-liquid system and to impurities (Shah et al.,1982). Abou-El-Hassan (1979) correlated a substantial amount of data with an expression that includes the effect of apparent viscosity. The correlation may be applied to gas-liquid-solid and gas-liquid-liquid systems.

Bubble rise velocity and bubble size distribution have a direct impact on the performance of bubble columns. Photographic techniques have been used widely for the study of such systems because of their simplicity (Schugerl et al.,1977; Akita and Yoshida,1974; Burchart and Deckwer,1975). Different statistical distribution functions have been found for bubble size by various workers. Akita and Yoshida (1974) found a logarithmic normal probability function, Buchart and Deckert (1975) found two different bubble size distributions coexisting in a column and Todtenhaupt (1971) a normal probability function. Though the original bubble size distributions differ markedly, the volume-surface mean drop diameter or Sauter mean diameter d_{vs} differ only slightly. The d_{vs} has been defined by Mugele and Evans (1951) as:

$$d_{vs}=\left(\Sigma\ n_i d^3_{pi}/\Sigma\ n_i d^2_{pi}\right) \qquad (2.6)$$

However, these mean sizes depend on coalescense and break-up of bubbles and obviously on the kind of flow in the column. The superficial gas velocity has been defined for the case of a bubble swarm by Sriram et al. (1977) as:

$$u_g=\varepsilon_g \int_0^{\infty} f(d_b)u(d_b)dd_b \qquad (2.7)$$

By writing the above equation for the case of a discrete function, the following expression can be obtained.

$$u_g=\varepsilon_g \frac{\Sigma\ n_i((i-1)\Delta d_b<d_b<i\Delta d_b)u_i((i-1)\Delta d_b<d_b<i\Delta d_b)}{\Sigma\ n_i((i-1)\Delta d_b<d_b<i\Delta d_b)} \qquad (2.8)$$

At low superficial gas velocities the dispersed gas moves freely as discrete bubbles in the liquid. This regime is known as uniform bubbling regime and has been studied by Molerus and Kurtin (1985). As the superficial gas velocity increases, the bubbles become unstable and localized liquid circulation is imposed on the flow field. Coalescense and break-up of bubbles can take place and there seems to be no regularity. This is the transition flow regime from the bubbling regime to the turbulence

regime and it has been explicitly treated by Maruyama et al. (1979). The turbulent flow regime which has been studied by Ueyama and Miyauchi (1979) is of practical importance. In this case, the circulation is clear in the column due to the existence of a phase rich in bubbles in the central plume of the column and a phase relatively lean in bubbles near the wall. Thus there exists a difference in buoyancy forces, which cause the circulation of the continuous phase. Provided that these conditions are met, isotropic turbulence theory can be applied once the length and velocity scales of the inertial subrange eddies are known.

2.4. Break-up and Coalescence of Drops in Turbulent Flow Fields-The Effect of Energy Dissipation

The intensity and structure of turbulence is of great importance, as it controls the fluid drop size and size distribution. A statistical description of the structure of turbulence originally proposed by Kolmogoroff (1941) provides a basis for describing fluid particle break-up and coalescence. Such phenomena play an important role in determining interfacial areas in hydrorefining processes (Shaw,1985) and in other multiphase systems where the mass transfer rates must be optimized.

The simplest form of turbulence is that of isotropic turbulence and has been defined by the condition that all mean values of functions of the flow variables should be independent of rotation and reflection of the axes of

reference (Taylor,1935; Taylor,1938). The turbulent eddies are divided into three categories. The energy-containing eddies which are of large wave numbers and depend on the characteristics of flow; The eddies of the inertial subrange which play the role of transfering the kinetic energy from the energy-dissipating eddies to the viscous eddies; and the energy-dissipating eddies, the smallest ones with respect to length scale, which are independent of the flow characteristics. The latter eddies depend on the energy lost from the large energy-containing eddies and once this energy rate is known their structure is determined. No matter how inhomogeneous the flow is, isotropic turbulent flow may be considered locally in the range of energy-dissipating eddies (Batchelor,1960). From dimensional reasoning, Kolmogoroff defined the length and velocity scales for the universal equilibrium range (inertial and viscous subranges) as:

$$\eta=(\nu^3/\varepsilon)^{1/4} \quad \text{and} \quad u=(\nu\,\varepsilon)^{1/4}$$

Where η is the length scale, u is the velocity scale, ν is the kinematic viscosity of the continuous liquid phase and ε is the energy dissipation rate per unit mass of liquid. The length scale L of the energy-containing eddies is comparable to the physical dimensions of the system. If d_p is the diameter of a drop and

$$\eta < d_p < L$$

then, the variation of dynamic pressure fluctuations in a distance equal to

d_p is strong enough to cause drop break-up. The maximum diameter of a drop, stable against break-up in turbulent flow fields is,

$$d_{max} \sim (\sigma/\rho)^{3/5} \varepsilon^{-2/5} \qquad (2.9)$$

and has been defined by Hinze (1955). However, there also exists a minimum drop size, stable against coalescence in turbulent flow fields which has been derived by Thomas (1981) as:

$$d_{min} \sim 2.4 \left(\frac{\sigma^2 h^2}{\mu \rho \varepsilon}\right)^{1/4} \qquad (2.10)$$

As d_{max} is over an order of magnitude greater than d_{min}, a broad range of drop sizes is stable in a turbulent field. This broad range narrows as the energy dissipation rate is increased. There exists a critical value of the energy dissipation ε_o where the d_{min} and d_{max} are theoritically the same (Thomas,1981). Therefore, if $\varepsilon < \varepsilon_o$ drops with diameters lying between d_{max} and d_{min} are too large to coalescence and also too small to be broken up. So, the final size distribution is controlled by the magnitude of the energy dissipation ε.

In agitated vessels, the energy dissipation rate, ε, is related to the impeller speed and vessel geometry:

$$\varepsilon = C\ D^2\ N^3 \qquad (2.11)$$

Where D is the diameter of the impeller, N is the number of revolutions of the impeller per unit time and C is a proportionality constant strongly depended on impeller type and size.

In tubular reactors for gas-liquid and gas-liquid-liquid systems the energy dissipation rate can be found approximately by ignoring the gas holdup and density of the gas

$$\varepsilon = u_g g \qquad (2.12)$$

A more accurate expression for calculating the energy dissipation rate in tubular reactors is derived in APPENDIX A.

2.5. Dispersion Phenomena in Agitated Vessels

Many operations in chemical engineering require the contact of two liquid phases. One of the most common methods of bringing about the contact of two liquid phases is to disperse drops of one within the other by mechanical agitation. The interfacial area is affected by the physical and chemical characteristics of the system and mechanical features of the equipment. These characteristics as well as their impact on the Sauter mean drop diameter in agitated vessels are presented in this section.

A number of investigators have presented correlations that relate drop sizes in agitated vessels to mixing parameters and physical properties of the system (Weinstein and Treybal,1973; Coulaloglou and Tavlarides, 1976; Nishikawa et al.,1987; Stamatoudis and Tavlarides,1985). Drop break-up

has been attributed to turbulent pressure fluctuations as discussed above. In agitated vessels, two distinct operating regimes have been observed. The Sauter mean drop diameter d_{vs} is controlled by different mechanisms in each of these regimes. At low impeller speeds drop break-up controls the Sauter mean diameter d_{vs} which is correlated as a function of energy dissipation, ε, to the power -0.4 (Weinstein and Treybal,1973; Nishikawa,1987). At high impeller speeds the dominant factor determining drop size is not break-up but the prevention of coalescence by the action of turbulence as discussed by Shinnar (1957, 1961) and Shinnar and Church (1960). This regime is known as coalescence prevention regime and the Sauter mean drop diameter was found to be proportional to the energy dissipation to the power -0.25 (Nishikawa,1987).

In agitated vessels, local mean drop diameter measurements have indicated that there exists a non-uniform drop size distribution. Smaller drops have been found to exist near the impeller (Weinstein and Treybal, 1973; Coulaloglou and Tavlarides, 1976). This is due to the fact that the energy is not dissipated uniformly over the volume of the vessel.

The effect of dispersed liquid volume fraction, ϕ, depends on the operating regime and its role becomes more significant in the coalescence-prevention regime (Nishikawa,1987). Generally, an increase of ϕ gives a larger Sauter mean drop diameter. However, it has to be pointed

out that the volume fraction, ϕ, has no effect on the Sauter mean diameter for lean dispersions less than 0.5% (Narshimhan,1980). The effect of relative viscosity, μ_d/μ_c, between dispersed liquid phase and continuous liquid phase has been found to have a considerable impact on the Sauter mean drop diameter. Nishikawa (1987) reported a power dependence of d_{vs} on μ_d/μ_c ranging from 0.125 to 0.25. Calderbank (1967) proposed a number of equations for d_{vs} including the term $(\mu_d/\mu_c)^{0.25}$. Hinze (1955) in his classical paper points out that the greater the deviation of relative viscosity is from unity the greater the resistance to drop break-up.

Unsteady-state drop size distributions in agitated vessels have been studied by Narsimhan et al. (1979,1980) and Ramkrishna (1974). The Sauter mean diameter changes relatively faster during the early stages of the operation and the rate of change may be correlated as an exponential function. Moreover, a change in the impeller speed also promotes a change of Sauter mean diameter in a comparatively small amount of time.

Nishikawa (1987) has summarized in the following equations the impact of physical properties of liquid phases and operating conditions on Sauter mean diameter:

$$d_{vs} = 0.0371\ \varepsilon^{-1/4}\ (d/D)^{3/4}\ (1+3.5\ \phi^{3/4})(\mu_d/\mu_c)^{13/40}\ (\sigma/\rho)^{3/8} \qquad (2.13)$$

(coalescence-prevention regime)

$$d_{vs} = 0.1050\ \varepsilon^{-2/5}\ (d/D)^{6/5}\ (1+2.5\ \phi^{2/3})(\mu_d/\mu_c)^{13/40}\ (\sigma/\rho)^{3/8} \qquad (2.14)$$

(break-up regime)

Where d is the diameter of the impeller and D is the diameter of the vessel. A detailed analysis reveals that the average power input per unit mass of liquid is not a satisfactory method of stirred vessel scale-up. Power is employed more advantageously by using a large impeller rotating at low speed rather than a short impeller at high speed. As it is shown from the above correlation there is a strong dependence of Sauter mean diameter on the geometry of the vessel. Therefore, it is an unreliable method to use Equations 2.13 and 2.14 for other geometrical arrangements.

2.6. Objectives

As it is shown in the literature review there is little information concerning gas-liquid-liquid systems. Therefore, there is a need for an extensive and detailed study of such systems. A number of different characteristics associated with phase interactions and hydrodynamics of gas-liquid-liquid systems will be addressed. The present investigation focusses on:

1. Gas Flux and Physical Properties of Dispersed Phase Liquid: since gas flux is directly related to energy dissipation rate, it is expected to play an important role in determining the mean drop size. Physical properties of dispersed phase liquid, including interfacial tension, viscosity and density,

are also expected to have a significant impact on the steady state mean drop size and drop size distribution.

2. Initial Drop and Bubble Size: different bubble sizes impose different shear fields which may result in different interfacial areas as is discussed for the case of agitated vessels (Section 2.5).

3. Unsteady State Drop Size Distribution: the transient drop size distribution is studied so that interfacial area can be modelled for reactions where steady state drop size distributions are not obtained.

4. Maximum and Minimum Stable Drop Sizes: drops stable against break-up and coalescence set bounds on the size spectrum of drops in a reactor. Formulae applicable to tubular reactors are derived. Such formulae are very useful for correlating the Sauter mean diameter.

5. Comparision between Tubular Reactors and Agitated Vessels: agitated vessels and tubular reactors are common phase-contacting devices. A comparision between them based on the rate of energy dissipation reveals their relative performance.

PART II

EXPERIMENTAL RESULTS

3.0. EXPERIMENTAL

3.1. Description of the Experimental Apparatus

All the experiments were carried out in a column with a rectangular cross-section of 15 X 30 cm in order to simulate an axial slice of a tubular reactor. A general schematic of the apparatus is shown in Figure 1. A detailed sketch of the column and gas chamber is shown in Figure 2. The rectangular cross-section was chosen to facilitate the photographic technique used in the present work. The thickness of the column is relatively large for such simulation. However, this was chosen to avoid wall effects. The column, 100 cm in height, was constructed of 0.635 cm thick sheets of perspex. Five taps of 1.27 cm diameter were drilled along the height of the column at 20 cm intervals, the lowest being 5 cm above the bottom plate so that the pressure drop could be measured. Compression fittings were used for the connections in order to avoid leaks. Five holes were drilled in the bottom plate of the column and fitted with interchangeable nozzles (0.15, 0.25, 0.35 and 0.5 cm diameter). The distance between the nozzles was 5 cm in order to avoid interactions between neighbouring bubbles, as they are generated.

The holes in the bottom plate linked the reactor to a gas chamber with a rectangular cross-section of 30 X 40 cm and height of 40 cm. This tank was made up of 0.635 cm thick sheets of perspex and had a top plate constructed of 1.27 cm thick sheet of perspex. A 25 X 2 cm slot and four capillaries

were drilled into the top plate to promote uniform gas distribution. The volume of the chamber was varied by filling it with water. This feature in conjuction with the various size nozzles permitted bubble generation at constant pressure, intermediate and constant flow conditions as discussed in section 2.2. A pressure relief valve set at 1.3 atm was used to prevent overpressuring the apparatus.

Two different rotameters were used to control the gas flow at low and high gas rates. At low gas rates, a 600 series rotameter of Matheson with a 15 cm tube (7632T) was used, equipped with a glass float. The typical flow range was from 6 cm^3/sec up to150 cm^3/sec. A high accuracy needle valve was placed at the inlet of the rotameter to get the downstream pressure close to atmospheric. The upstream pressure was less than 138 kPa, as specified by the rotameter manufacturer. At high gas rates a Fischer & Porter rotameter was used with a typical flow range from 100 cm^3/sec up to 1750 cm^3/sec. Calibration curves for both rotameters are shown in Figure 3.

Cylinder air was used to generate bubbles and a two-stage brass regulator Matheson (Model 8) was used to control the pressure. The delivery pressure gauge could be varied in the range of 0-690 kPa. A copper-pipe 6 cm I.D. and 60 cm long was used to saturate the air with water in order to avoid mass transfer in the column. The saturator was filled with the same liquid as the continuous liquid phase.

U-glass-tube manometers 0.5 cm I.D. were used for the following purposes:

-To measure the pressure fluctuations under the gas-distributor plate because of the bubble generation.

-To measure the pressure in the gas chamber.

-To measure the pressure at the outlet rotameter.

-To measure the pressure along the column.

A single experimental setup was devised to generate various drop sizes. The device comprised a 2 lit volume flask as a tank for the dispersed phase liquid, three liquid distributors with orifice sizes (0.32, 0.16, 0. 8 cm) and a valve to control the liquid flow rate.

3.2. Experimental procedure

The reactor was operated in batch mode with respect to both continuous and dispersed phase liquids and in continuous mode with respect to gas phase. The physical properties of various G-L-L systems used for this investigation are listed in Table 1. Sources and purities of these chemicals are tabulated in Table 2. Viscosity was measured using an Ostwald viscometer and interfacial tension was measured using a ring intertensiometer. During a typical experiment, the column was filled with distilled water to a depth of 85 cm and air was passed through the nozzles at a flow rate ranging from 45 to 1750 cm^3/sec. A perforated plate was placed at the top of the reactor and about 5 cm below the water level in

order to minimize free surface effects. The dispersed phase liquid was introduced from the top of the reactor through various size nozzle distributors (0.32, 0.16 or 0.1 cm). The initial drop size was greater than 2000 μm. Drop and bubble diameters were determined photographically using a Nikon camera (Shutter speed 1/1000th sec) in conjuction with an image analyzer (Bausch and Lomb, Omnicon-3000 with NOVA-4 data general). At low gas fluxes, photographs were taken while the column was operating. However, at higher gas fluxes photographs were taken only at the end of an experiment. To study the dependence of drop size on time at high gas fluxes the following procedure was used. After stopping the air supply at fixed time intervals, photographs were taken immediately and the experiment was repeated all over again in order for photographs to be taken at the next fixed time interval. Preliminary experiments showed that the mean drop diameter remained virtually constant after 15 minutes of operation. A typical image analysis was based on the size analysis of 1000 plus drops. Size analysis of approximately 500 drops gave similar results. Correction factors had to be used due to geometrical magnifications involved in photographic techniques. The repeatability of the above described experimental procedure is within 5% as shown in Table 3.

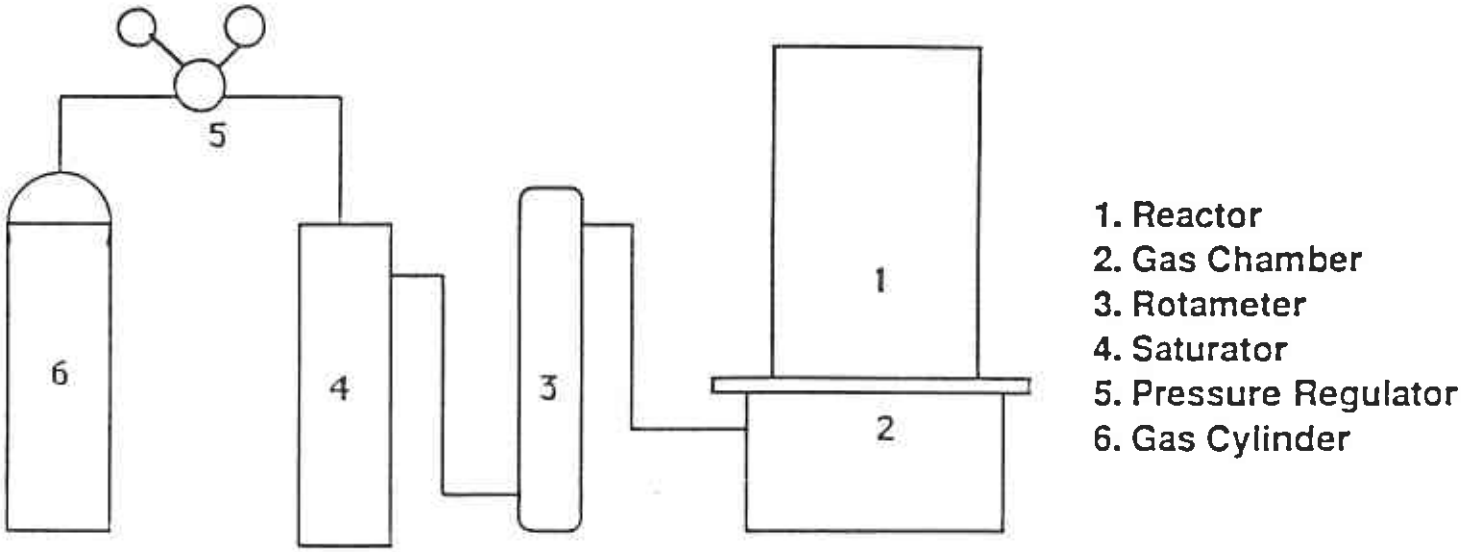

Figure 1: Schematic diagram of experimental apparatus

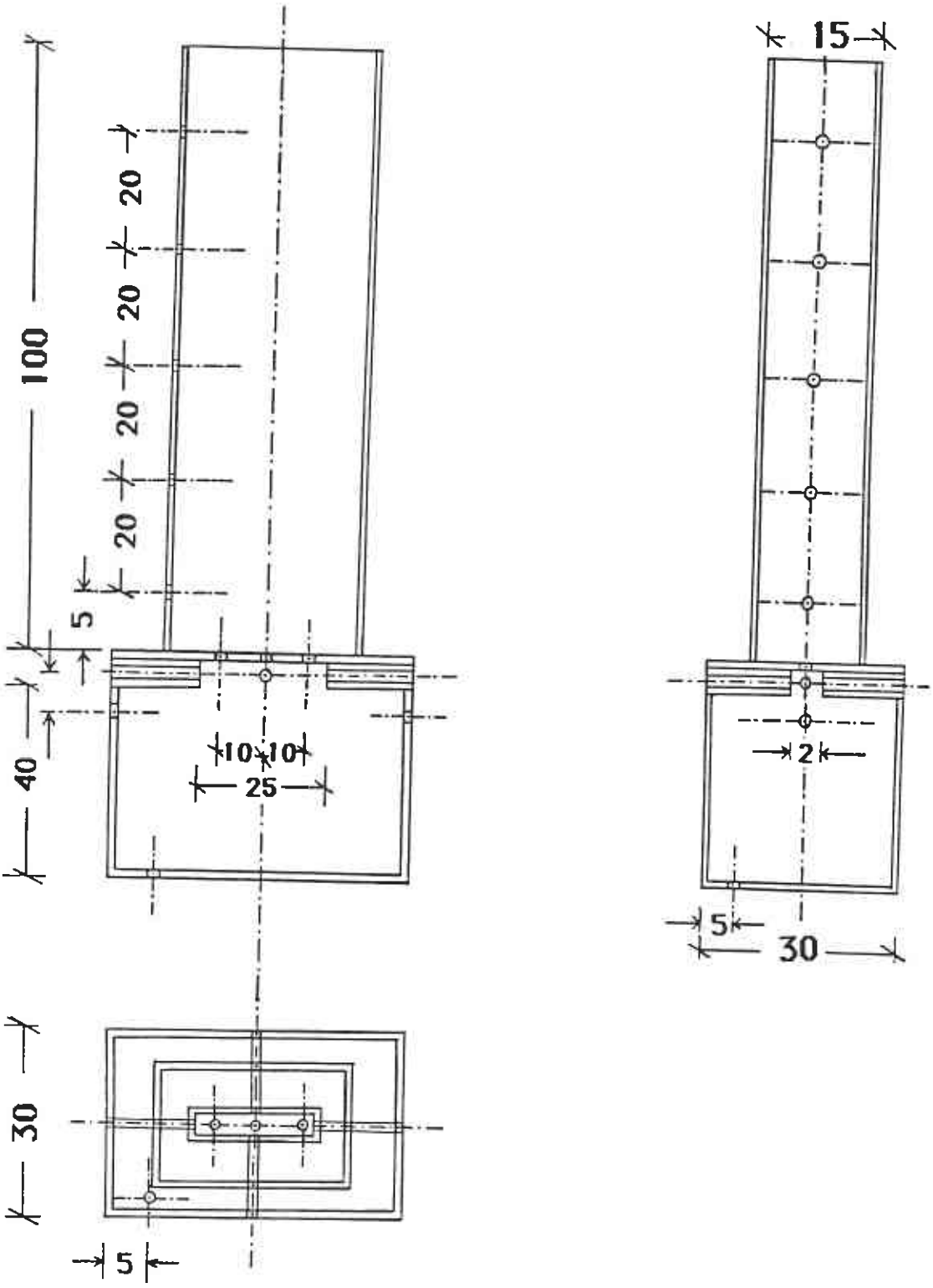

Figure 2: Detailed sketch of bubble column and gas chamber

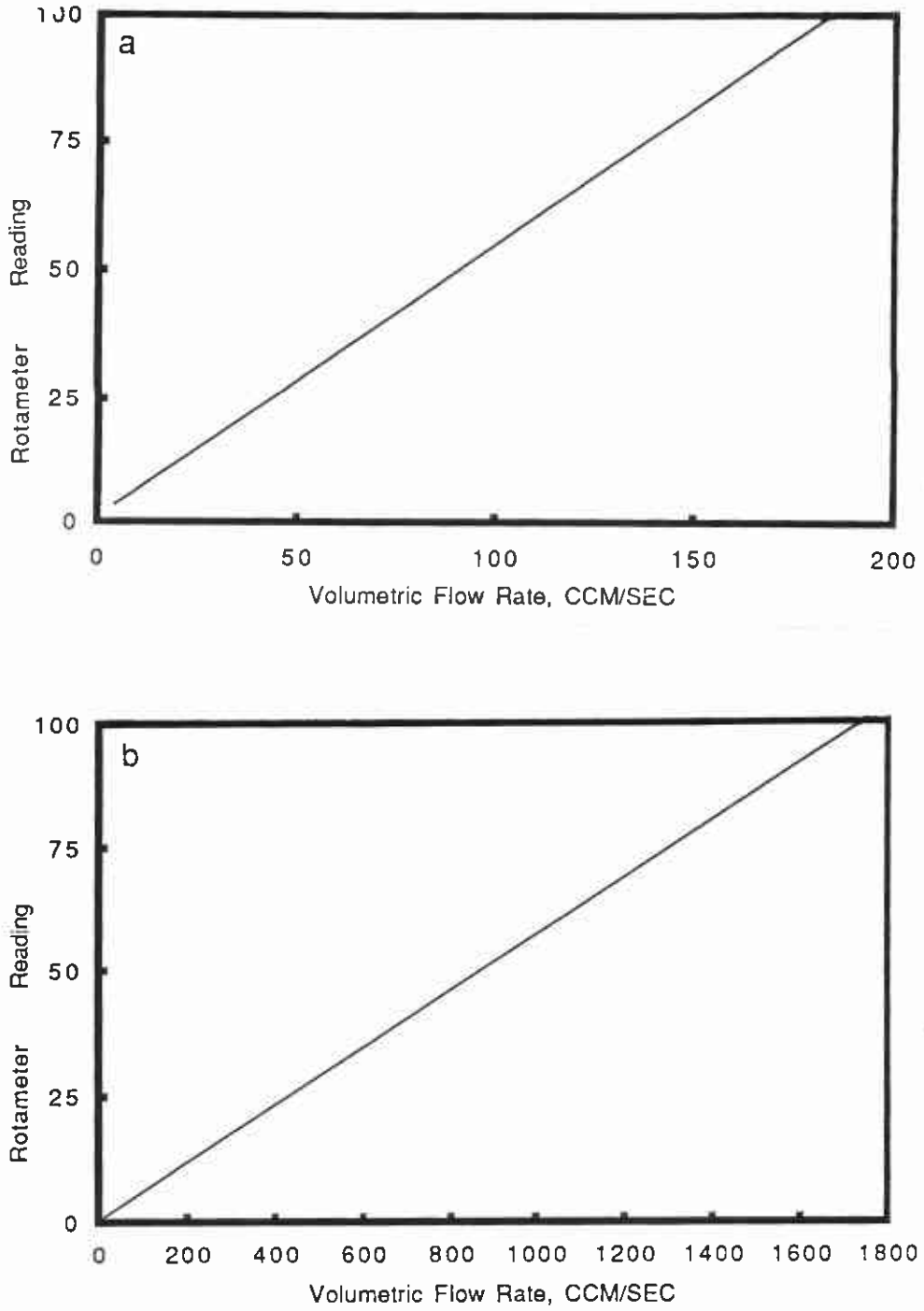

Figure 3: Calibration curves for the rotameters: a) Matheson (7632T) b) Fischer & Porter

TABLE 1. Physical properties of Gas-liquid-liquid systems.

Systems	μ_d, poise	σ, dyne/cm	ρ_d, g/cm^3
A. Linseed oil (96%v)+TCE (4%v) Water-Air	0.25	6.1	0.95
B. Linseed oil (85%v)+TCE (15%v) Water-Air	0.17	6.2	1.00
C. Linseed oil (82%v)+TCE (18%v) Water-Air	0.15	6.4	1.02
D. Linseed oil (78%v)+TCE (22%v) Water-Air	0.13	6.8	1.04
E. Linseed oil (61%v)+TCE (39%v) Water-Air	0.03	10.2	1.13
F. Cottonseed oil (83%v)+TCE (17%v) Water-Air	0.19	23.6	1.00
G. Dibenzyl Ether-Water-Air	0.05	5.1	1.04

Systems B, F and G are referred to as the linseed oil, cottonseed oil and dibenzyl ether systems respectively in the text. Systems A, C, D and E have only been used to quantify the impact of relative density and viscosity.

TABLE 2. Sources and Purities of Chemicals

Chemicals	Purity (%)	Source
Air	99	CANOX
Water	High purity	U. of TORONTO Dept. of Chem. Eng.
Linseed oil	-	RECOCHEM
Cottonseed oil	For laboratory use	FISCHER Scientific Company
Dibenzyl ether	98	FLUKA AG (Switzerland)
Trichloroethylene	99	BDH Chemicals

TABLE 3. Repeatability of the Procedure.

System	D_{max}, µm	D_{vs}, µm	D_{min}, µm	u_g, cm sec^{-1}	ϕ(%)
B	926	465	76	0.1	0.45
	945	472	78	0.1	0.45
A	1051	520	88	0.1	0.45
	1055	505	83	0.1	0.45
F	521	262	43	0.4	0.45
	532	269	49	0.4	0.45
G	545	274	45	0.2	0.45
	529	279	49	0.2	0.45

The maximum deviations which can be observed from the above listed results vary from 2% to 5%.

PART III

RESULTS AND DISCUSSION

4.0. RESULTS

In this section the results obtained in the present investigation are presented in the form of Tables and Figures. These results are discussed in chapter 5.

Table 4 shows the maximum, minimum and Sauter mean diameters of dispersed phase drops for the bulk of experiments carried out in the present investigation. The operating conditions and systems used are also shown.

Figure 4 shows the gas holdup in gas-liquid-liquid tubular reactors. On the same Figure the generalized correlation of Abou-El-Hassan (1979) is shown which is valid for two and three phase systems. Kato's correlation (1984) is also sketched on the same Figure for gas-liquid-liquid tubular reactors operating in a continuous fashion with respect to all phases. Figures 5 and 6 are typical examples of size distributions and cummulative drop size distributions of dispersed phase droplets respectively for a variety of operating conditions and systems.

4.1. Unsteady State Drop Size Distributions

Figures 7, 8 and 9 illustrate unsteady state cummulative volume distributions for various systems and operating conditions used in this investigation. Figures 10, 11 and 12 show the effect of superficial gas velocity, interfacial tension and viscosity on the rate at which steady state

is reached in three phase tubular reactors. Figures 13 and 14 are plots of drop diameter against time for various cummulative volume values. These Figures are based on Figures 7,8 and 9 and are very helpful in identifing the similarity variable (Section 5.3.2). Figures 15 and 16 show the significance of the similarity variable. Finally Figure 17 is a comparision between the rate at which steady state drop size distributions are approached in tubular reactors and agitated vessels.

4.2. Steady State Drop Size Distributions

Figure 18 shows the effect of superficial gas velocity on the Sauter mean diameter of dispersed liquid drops for three different systems. The results are correlated (Equation 5.16) and a parity plot for this correlation is shown in Figure 19. The functional dependence of maximum and minimum stable drop sizes against break-up and coalescence respectively are shown on Figures 20 and 21 for two different systems. The various slopes appearing on Figures 20 and 21, calculated by using least square method, are tabulated in Table 5. Figures 22, 23, 24 and 25 show the effect of energy dissipation rate on the breadth of the drop size distribution for various systems.

Figure 26 shows the effect of relative viscosity on the steady state drop size. Figures 27 and 28 show the effect of dispersed phase volume fraction on the steady state Sauter mean diameter for two different

systems. In Table 6, the effect of density difference between the two liquid phases is shown.

Finally, Figure 29 shows a comparision of the relative performance of tubular reactors (experimental data) and agitated vessels (Equations 2.13 and 2.14) for three different systems:

-a system with high interfacial tension and high relative viscosity

-a system with low interfacial tension and high relative viscosity

-a system with low interfacial tension and low relative viscosity.

TABLE 4. Steady state Max, Min and Sauter Mean Diameters.

System	D_{max}, μm	D_{vs}, μm	D_{min}, μm	u_g, cm sec^{-1}	ϕ(%)
B	926	465	76	0.1	0.45
	788	396	65	0.2	0.45
	563	283	46	0.3	0.45
	525	264	43	0.4	0.45
	418	210	34	1.0	0.45
	358	180	29	2.0	0.45
	299	150	25	3.9	0.45
	961	483	79	0.1	0.10
	531	267	44	0.4	0.10
	365	185	32	2.0	0.10
	1011	508	83	0.1	1.00
	573	288	47	0.4	1.00
	410	205	31	2.0	1.00
	1240	623	102	0.1	3.00
	665	334	55	0.4	3.00
	475	240	38	2.0	3.00
F	1198	602	98	0.1	0.45
	832	418	68	0.2	0.45
	605	304	50	0.3	0.45
	521	262	43	0.4	0.45
	448	225	37	1.0	0.45
	368	185	31	2.0	0.45
	328	165	27	3.9	0.45
	1171	597	98	0.1	0.10
	549	276	45	0.4	0.10
	360	183	30	2.0	0.10
	1193	619	92	0.1	1.00
	625	314	51	0.4	1.00
	1201	635	96	0.1	3.00
	649	340	61	0.4	3.00
	499	250	42	2.0	3.00
G	637	320	52	0.1	0.45
	545	274	45	0.2	0.45
	482	242	40	0.4	0.45
	524	263	43	0.1	0.10
	629	316	52	0.1	1.00
	490	246	40	0.4	1.00

TABLE 5. Slopes of Various Systems in Both Flow Regimes

	Slopes in Low Gas Flux flow Regime		Slopes in High Gas Flux Flow Regime	
System	Max	Min	Max	Min
B	0.48	0.47	0.25	0.24
F	0.54	0.55	0.24	0.24
G	0.22	0.21	0.22	0.21

TABLE 6. Effect of relative density ρ_{ld}/ρ_{lc}

System	ρ_{ld}/ρ_{lc}	μ_d/μ_c	σ, dyne/cm	u_g, cm/sec	d_{vs}, μm	$d_{vs,cor.}$, μm
A	0.95	25	6.1	0.1	520	441
B	1.00	17	6.2	0.1	465	434
C	1.02	15	6.4	0.1	459	442
D	1.04	13	6.8	0.1	430	430
B	1.00	17	6.2	0.2	396	383
E	1.13	3	10.2	0.2	302	432
B	1.00	17	6.2	0.4	264	246
D	1.04	13	6.8	0.4	252	252
E	1.13	3	10.2	0.4	202	291

$d_{vs,cor.}$ is the corrected value of Sauter mean diameter accounting for the different relative viscosity μ_d/μ_c of various systems. Basis is taken μ_d/μ_c=13.

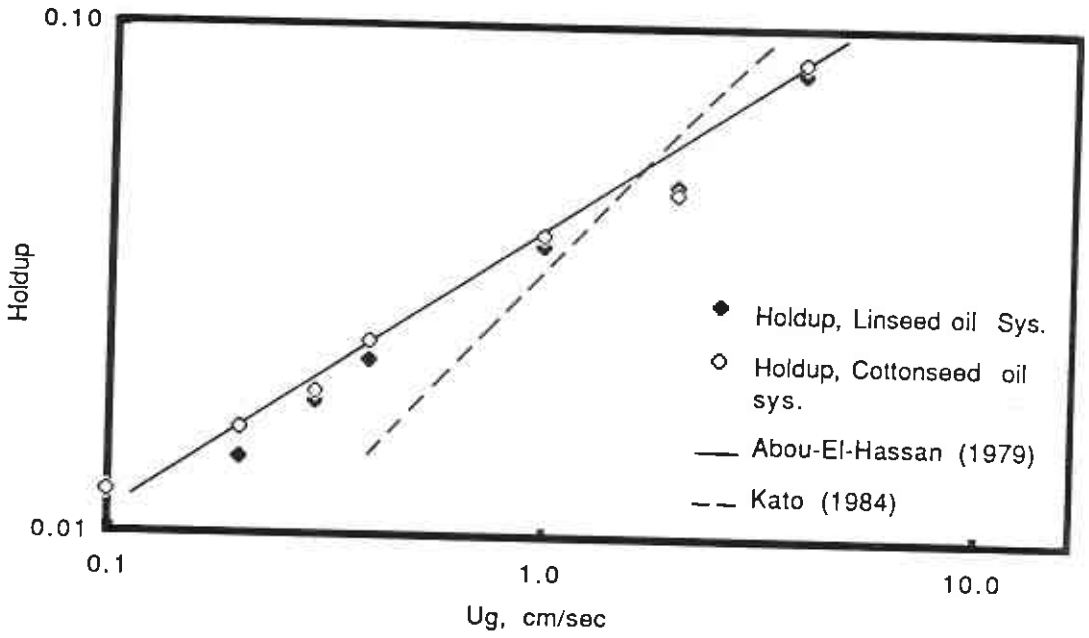

Figure 4: Gas holdup in three phase tubular reactors

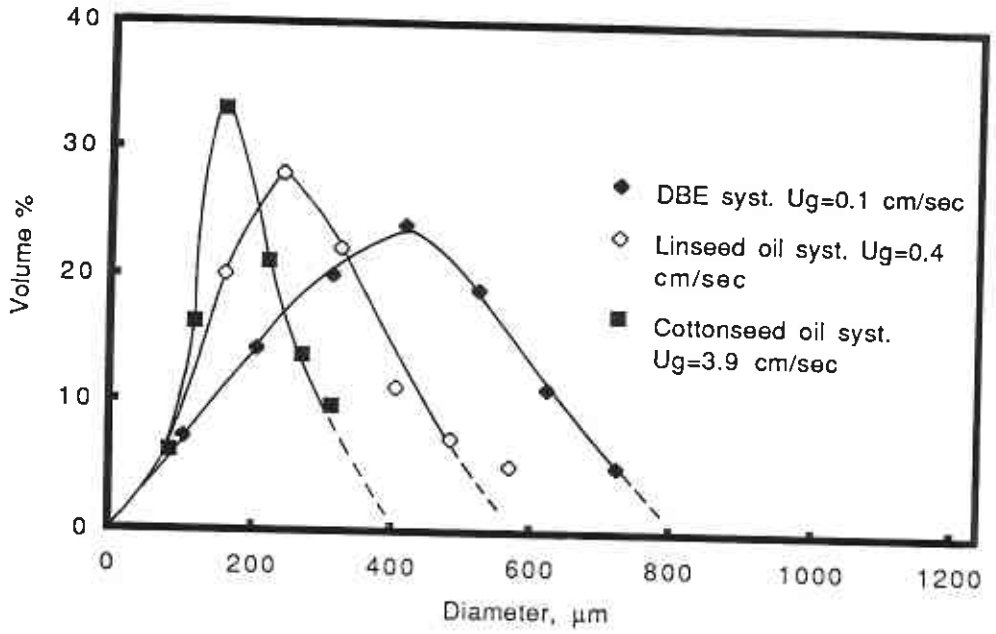

Figure 5: Sample size Distributions for dispersed phase drops

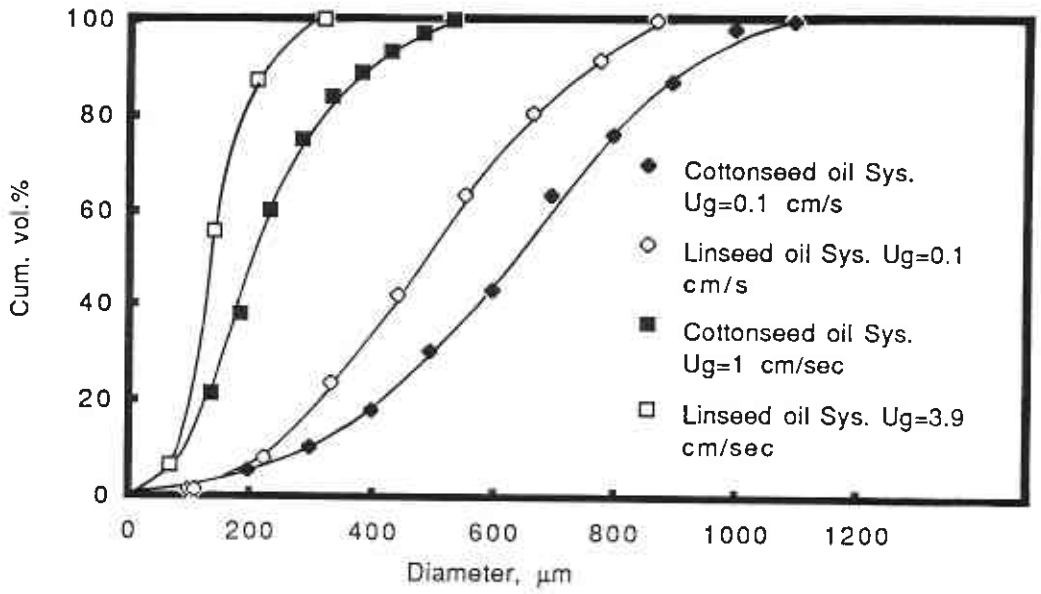

Figure 6: Sample cumulative drop size distributions

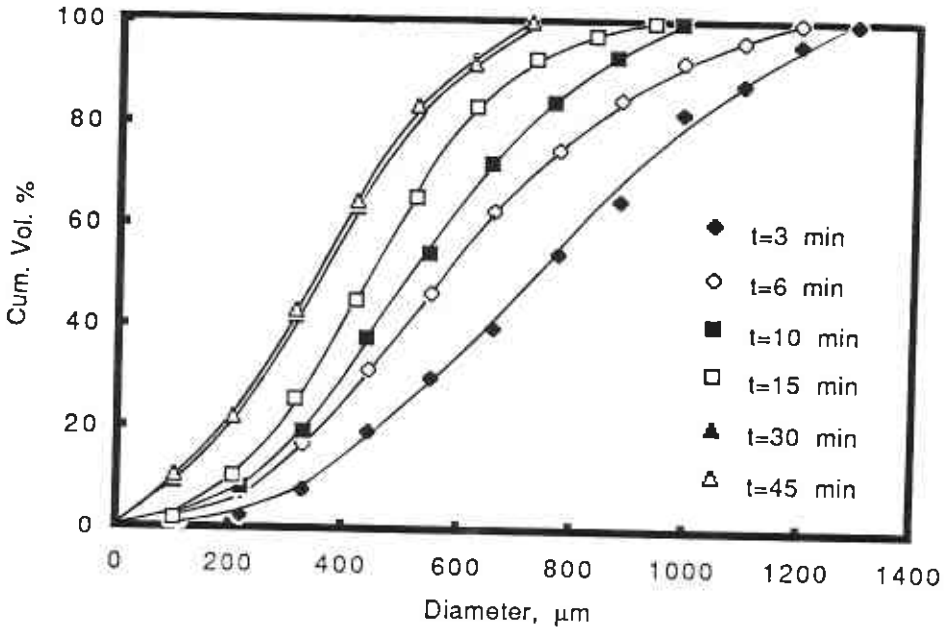

Figure 7: Unsteady state cumulative volume distributions for the dibenzyl ether system (u_g=0.1 cm/sec)

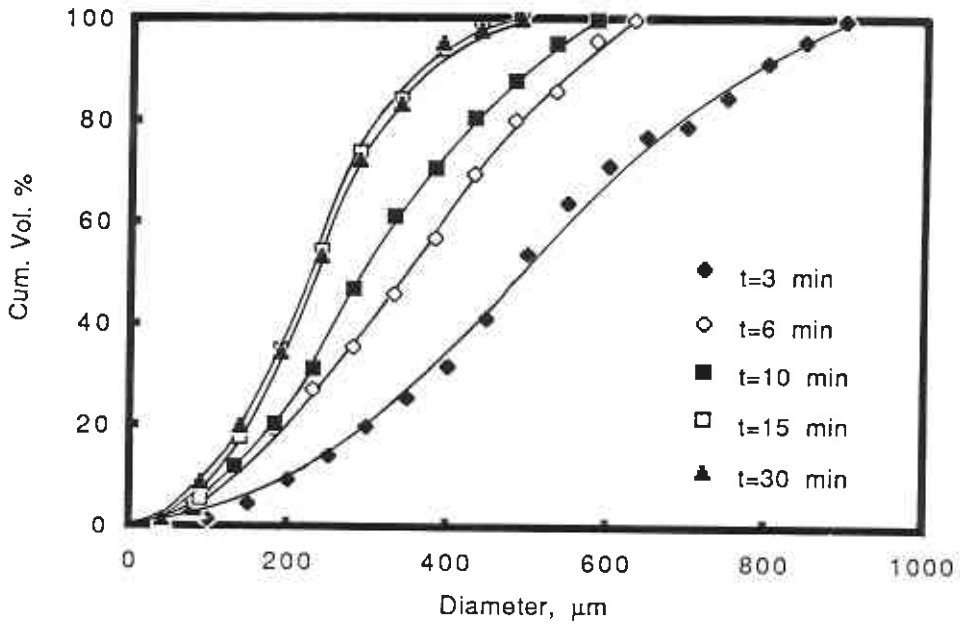

Figure 8: Unsteady state cumulative volume distributions for the cottonseed oil system (u_g=0.4 cm/sec)

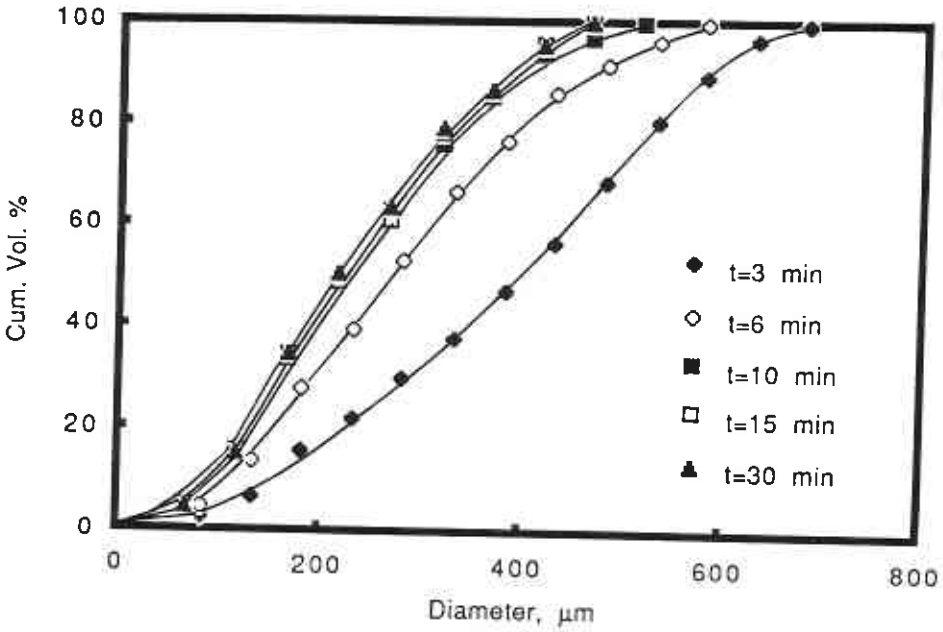

Figure 9: Unsteady state cumulative volume distribution for the linseed oil system (u_g=2 cm/sec)

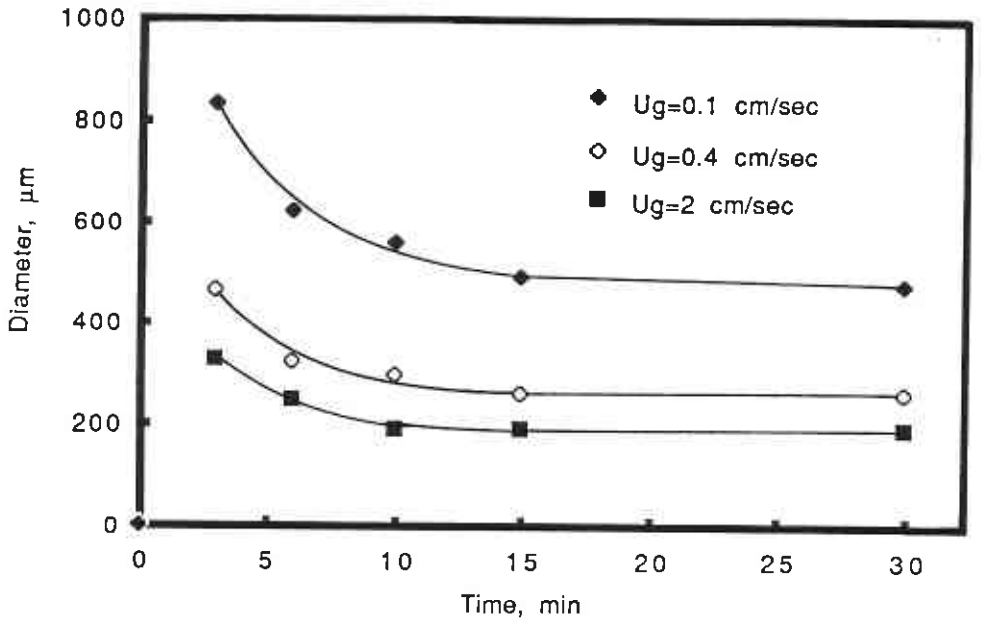

Figure 10: The effect of superficial gas velocity, u_g, on the unsteady state mean drop size (linseed oil system)

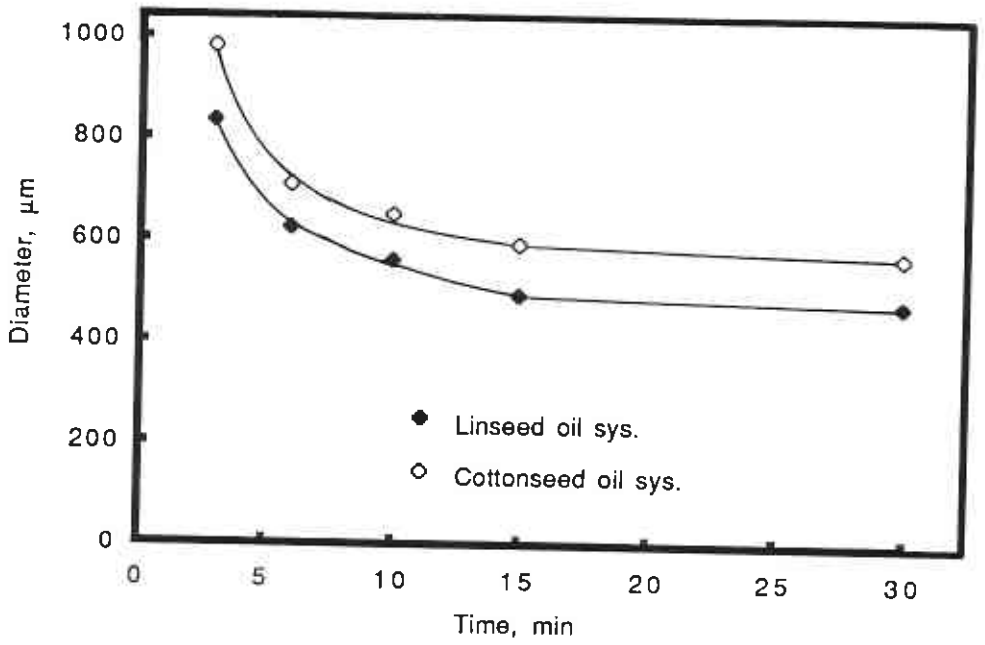

Figure 11: The effect of interfacial tension, σ, on the unsteady state mean drop size (u_g=0.1 cm/sec)

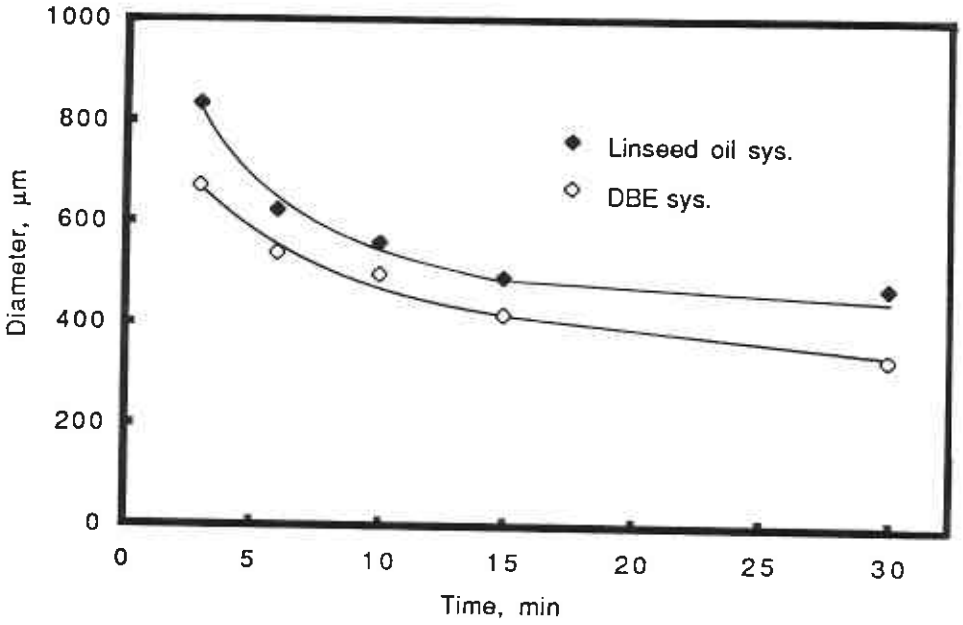

Figure 12: The effect of relative viscosity, μ_d/μ_c, on the unsteady state mean drop size (u_g=0.1 cm/sec)

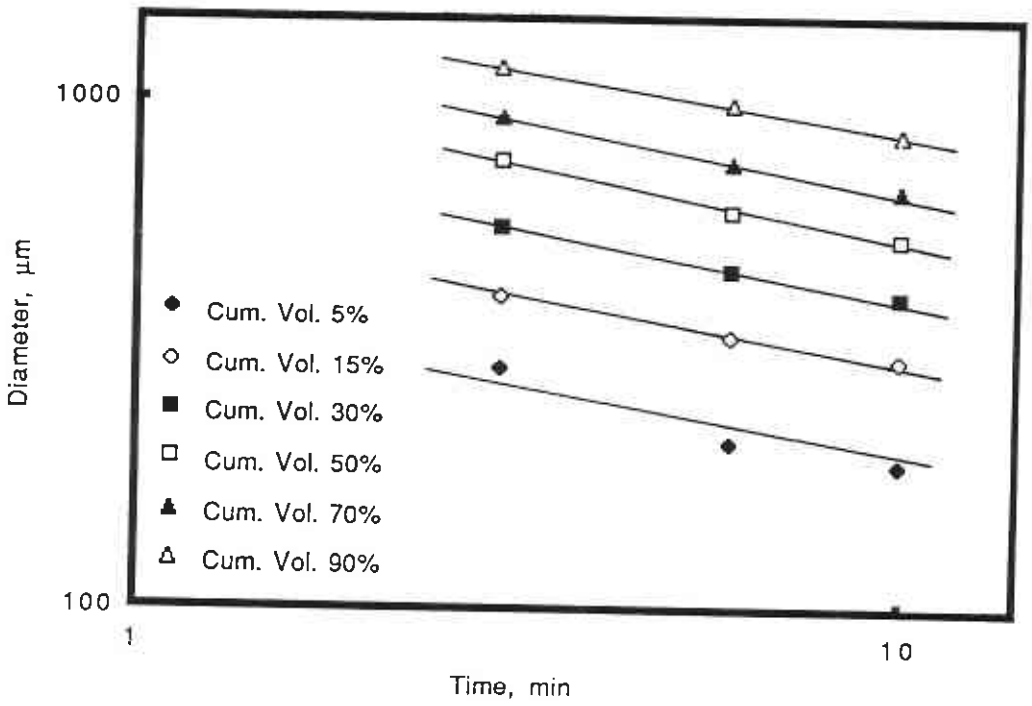

Figure 13: The functional dependence of the transition probability function $\Gamma(v)$ on drop size (dibenzyl ether system, u_g=0.1 cm/sec)

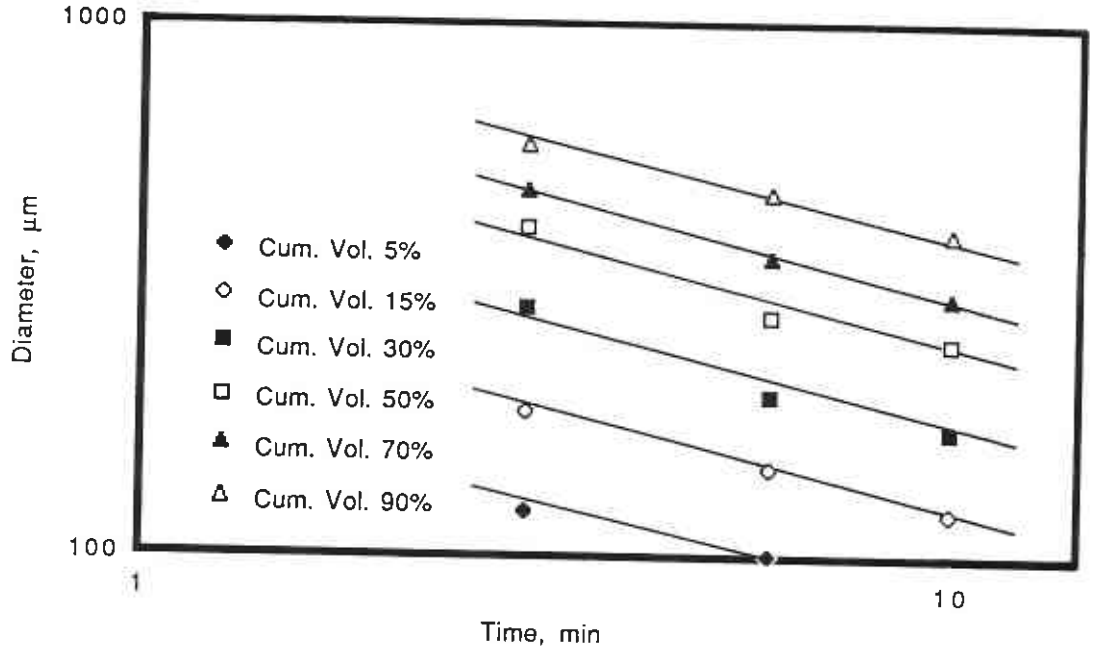

Figure 14: The functional dependence of the transition probability function $\Gamma(v)$ on drop size (linseed oil system, u_g=2 cm/sec)

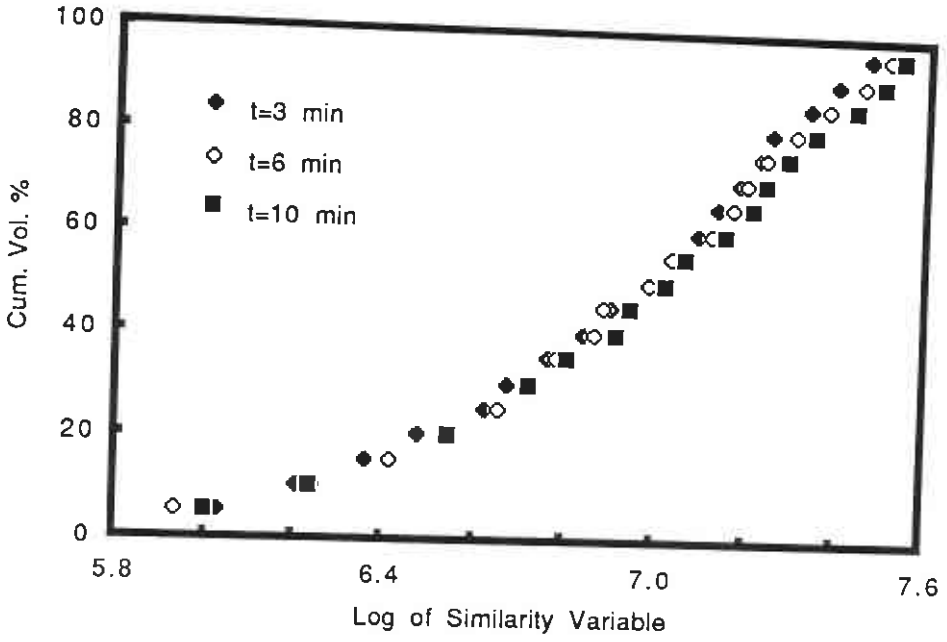

Figure 15: The similarity of the unsteady state cumulative volume size distributions (dibenzyl ether system, u_g=0.1 cm/sec)

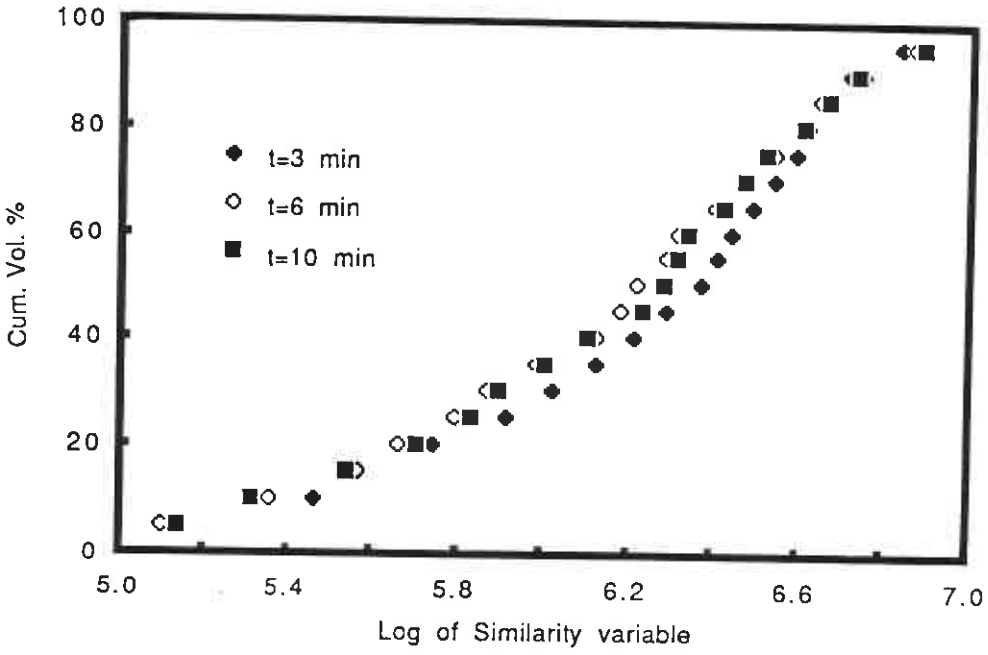

Figure 16: The similarity of the unsteady state cumulative volume size distributions (linseed oil system, u_g=2 cm/sec)

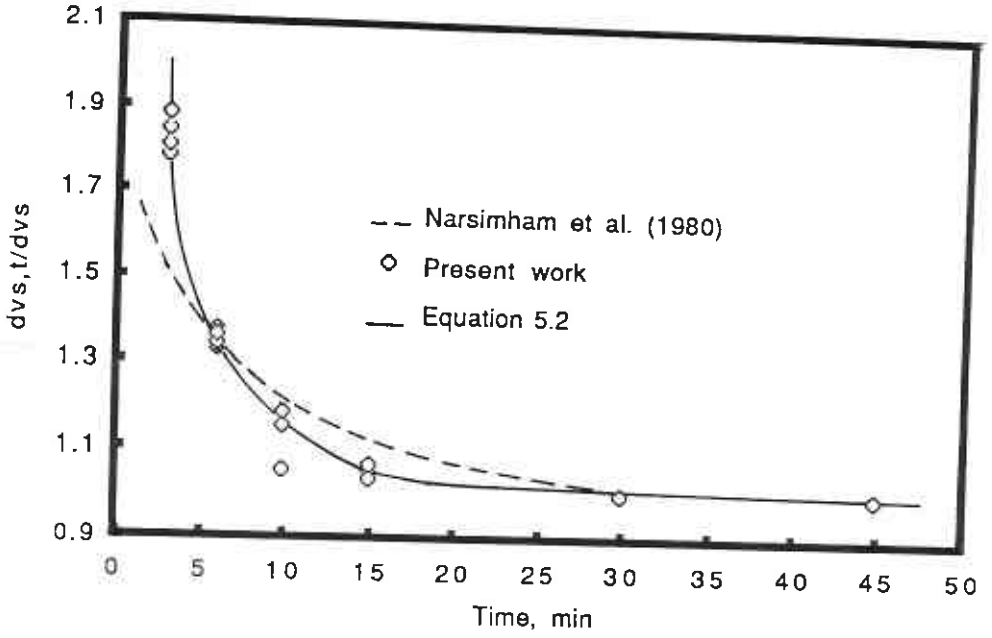

Figure 17: A comparision between the rate at which steady state drop size distributions are approached in tubular reactors and agitated vessels

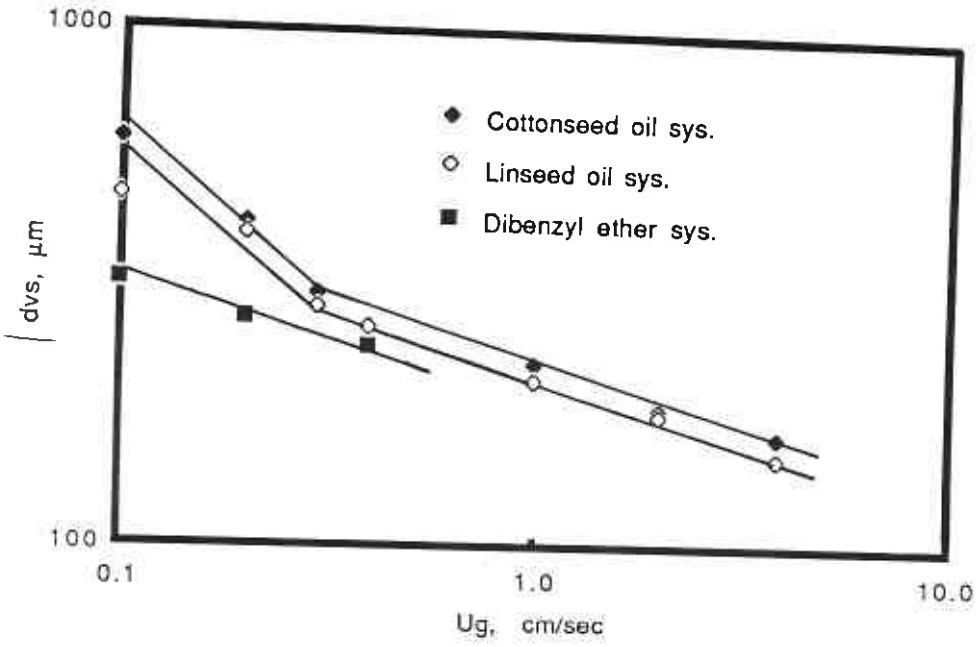

Figure 18: The effect of superficial gas velocity on the steady state Sauter mean diameter of dispersed liquid drops

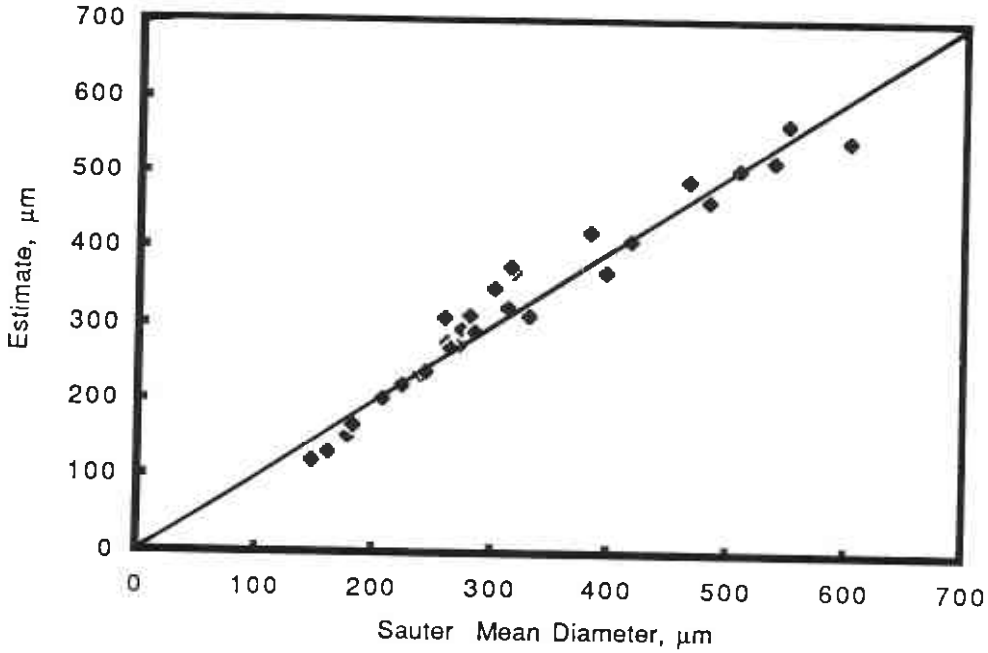

Figure 19: Parity plot for Equation 5.16

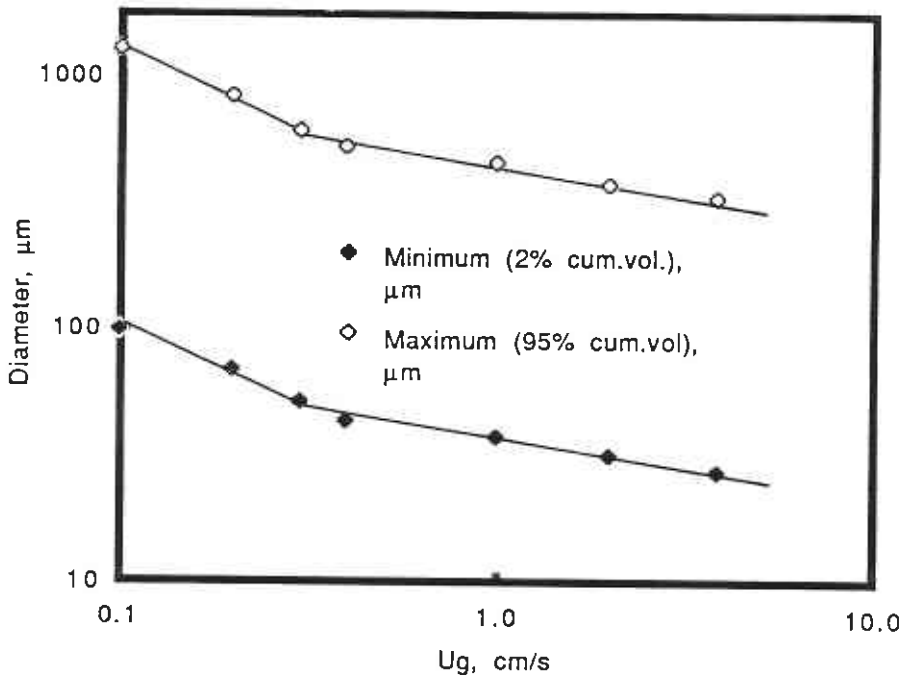

Figure 20: The dependence of maximum and minimum drop sizes on the energy dissipation rate (cottonseed oil system)

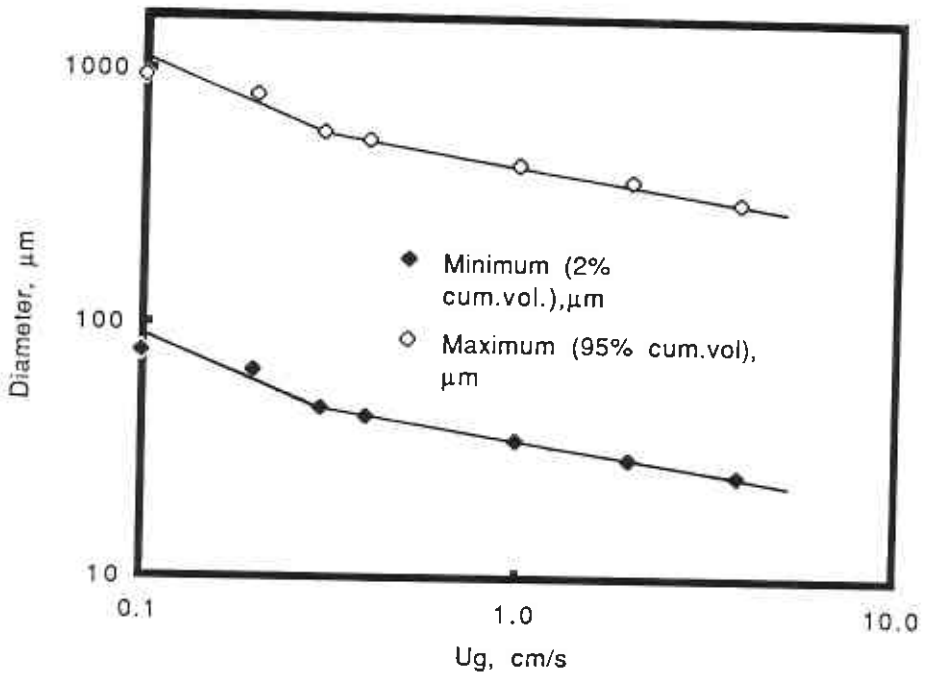

Figure 21: The dependence of maximum and minimum drop sizes on the energy dissipation rate (linseed oil system)

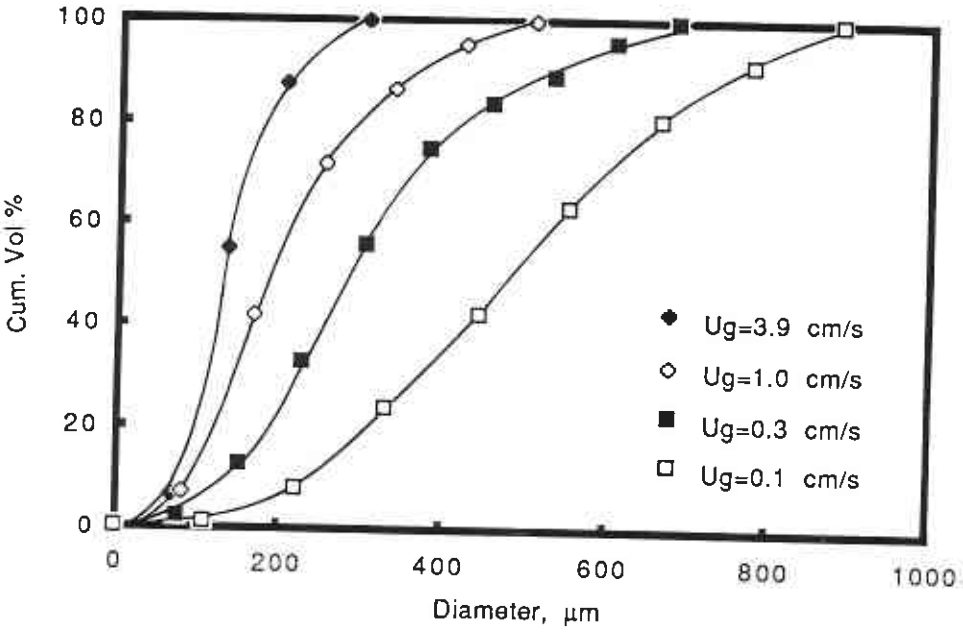

Figure 22: The effect of energy dissipation rate on the breadth of drop size distributions for the linseed oil system

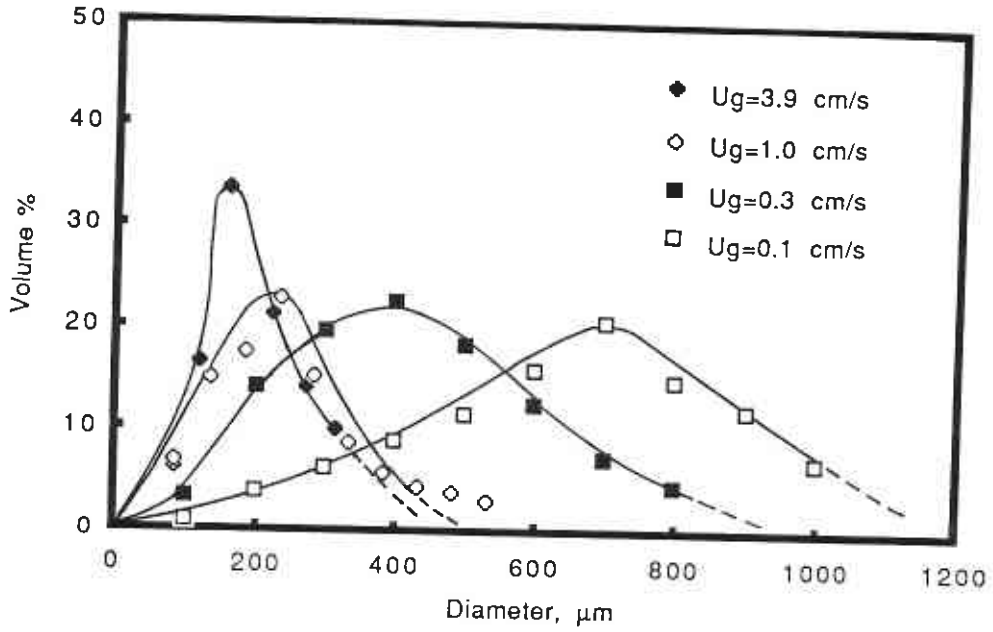

Figure 23: The effect of energy dissipation rate on the breadth of drop size distributions for the cottonseed oil system

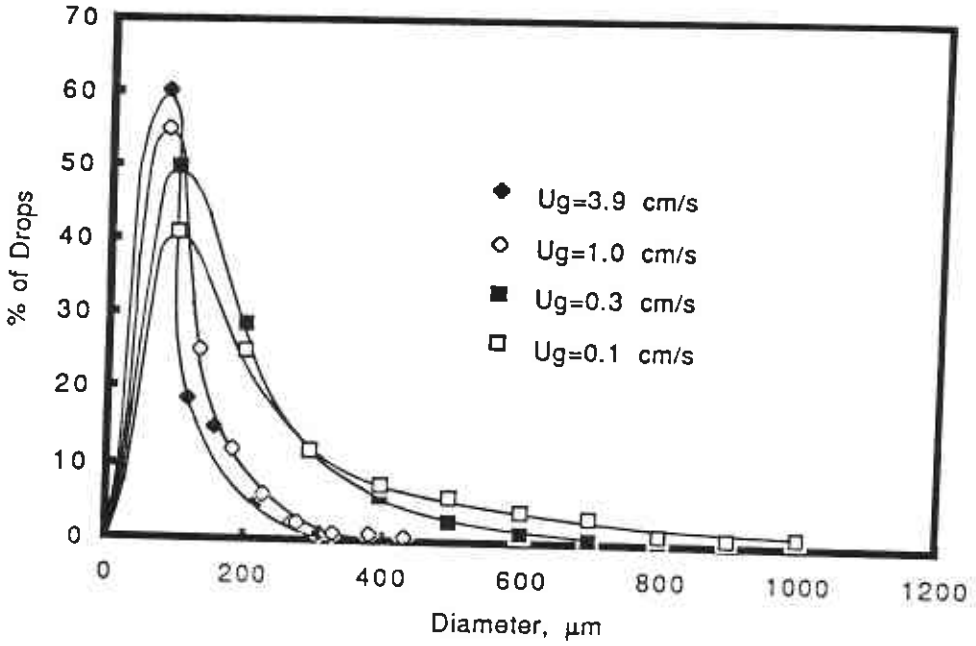

Figure 24: The effect of energy dissipation rate on the size spectrum of dispersed phase drops (cottonseed oil system)

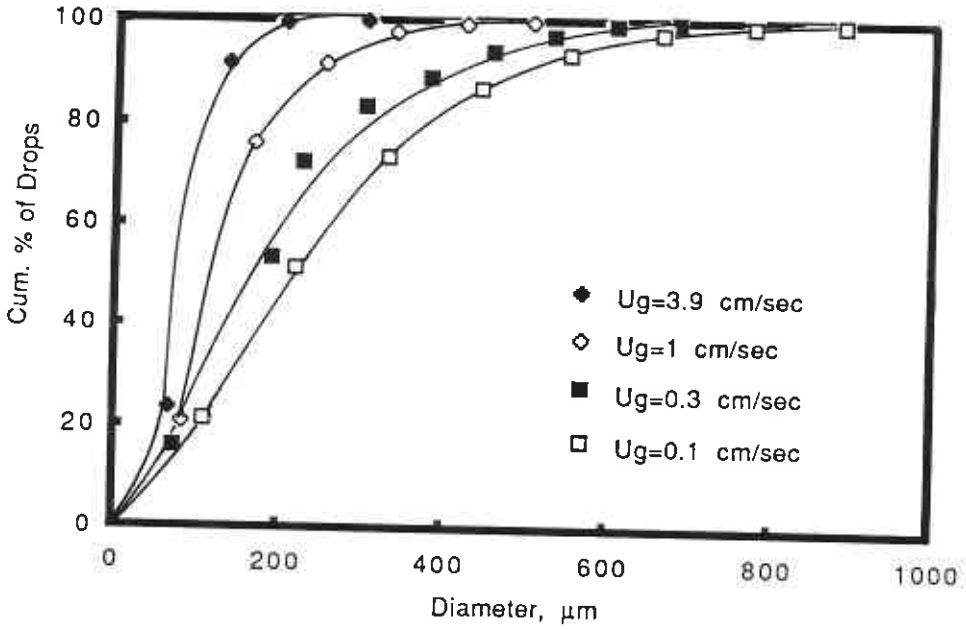

Figure 25: The effect of energy dissipation rate on the cumulative size spectrum of dispersed phase drops (linseed oil system)

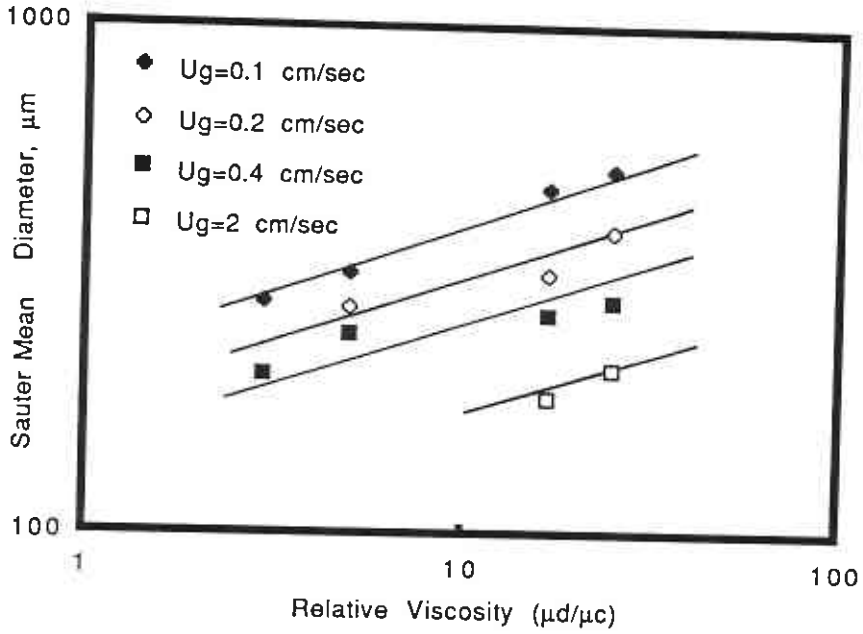

Figure 26: The effect of relative viscosity, μ_d/μ_c, on the steady state Sauter mean drop size

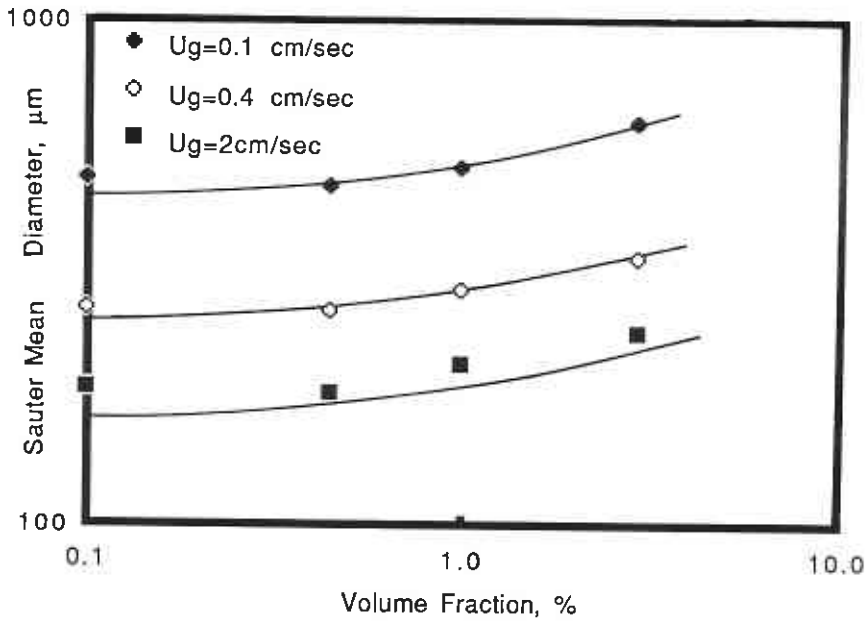

Figure 27: The effect of volume fraction,ϕ , of the dispersed phase on the steady state Sauter mean diameter (linseed oil system)

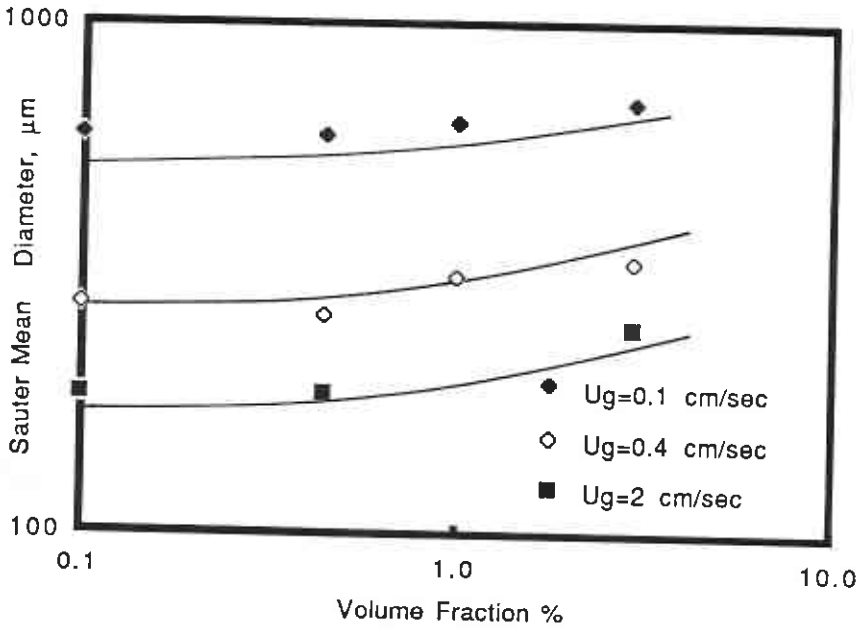

Figure 28: The effect of volume fraction, ϕ, of dispersed phase on the steady state Sauter mean diameter (cottonseed oil system)

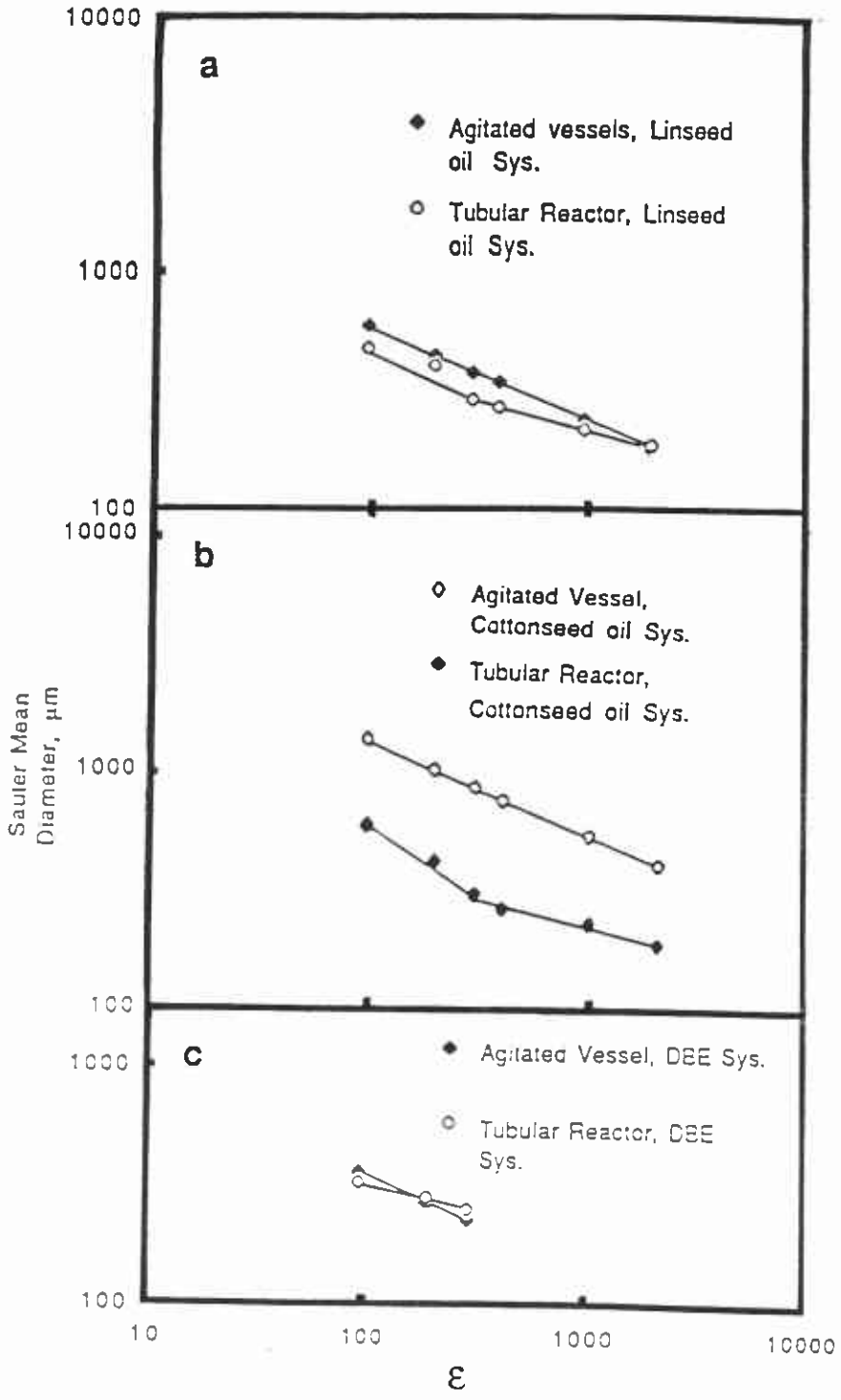

Figure 29: A comparision of the performance of tubular reactors (experimental data) and agitated vessels (Equations 2.13 and 2.14 with d/D=0.5) at: a) high relative viscosity and low interfacial tension, b) high relative viscosity and high interfacial tension, c) low relative viscosity and low interfacial tension

5.0. DISCUSSION

The results obtained in this investigation are presented in chapter 4 in the form of Tables and Figures. In this chapter these results are discussed and some characteristics not obviously extracted from the Figures are presented and explained. Gas holdup as a hydrodynamic parameter characterizing the operation of gas-liquid-liquid tubular reactors is discussed first. Then, unsteady state drop size distributions and unsteady state mean drop size are presented as fundamental variables in characterizing the time dependence and transition of drop breakage in these processes. Subsequently, the importance of Sauter mean drop diameter in estimating the interfacial area as well as the size spectrum of stable drops, are discussed and correlated. The impact of physical properties of the dispersed liquid phase on Sauter mean diameter is assesed and quantified in conjuction with the impact of superficial gas velocity. Finally, the results of this investigation are compared with stirred tank analogues.

5.1. Gas Holdup

Figure 4 shows the relationship between gas holdup and superficial gas velocity in the reactor. The mean gas holdup ε_g is correlated as:

$$\varepsilon_g = 0.375\, u_g^{0.575} \qquad (5.1)$$

where u_g is expressed in the units of cm/s. Shah et al. (1982) in a review

paper pointed out that the gas holdup depends mainly on superficial gas velocity and is often very sensitive to the kind of liquid media for gas-liquid systems. The number of correlations proposed indicates that no single unified equation is available. However, the exponents of u_g in most of the proposed correlations particularly for churn turbulent flow are very close to 0.5 (Ueyama and Miyauchi, 1979).

As seen in Figure 4, the gas holdup in the range of 0.1-4 cm/s for linseed oil and cottonseed oil systems are similar indicating that the physical properties of the dispersed liquid phase do not have a significant effect. These values are comparable to values given by Abou-El-Hassan (1979), who devised a generalized correlation for gas holdup in gas-liquid and gas-liquid-solid bubble columns. The presence of a dispersed phase leads to a reduction in gas holdup vis-a-vis corresponding gas-liquid system. Kato et al. (1972) and Nakamura (1978) observed a similar reduction in gas holdup in bubble columns containing suspended solid particles. Ying et al. (1980) and Vasalos et al. (1980) investigated the effect of solids concentration and concluded that an increase in solid concentration generally decreases the gas holdup. This reduction in gas holdup has been attributed to an increase in the apparent viscosity of the bulk liquid resulting from the presence of a dispersed phase (Abou-El-Hassan, 1979) and would appear to be indepedent of the physical properties of the dispersed phase. Results obtained as part of this study are consistent with this finding as indicated in Figure 4. Kato et al. (1984)

found that gas holdup in gas-liquid-liquid systems tended to be 10-15% lower than values encountered in gas-liquid systems. Their correlation (dashed line in Figure 4) severely underestimates gas holdup in gas-liquid-liquid columns at low gas fluxes and overestimates it at high gas fluxes. However, the operation of their column was continuous with respect to all three phases. In batchwise operation the liquid in the wake of bubbles moves faster than the continuous liquid phase. As a result, the average velocity of the bulk liquid phase decreases. Since gas holdup is increased with the bulk liquid velocity, a slightly higher holdup is observed in cocurrent continuous operation.

5.2. Drop Size Distribution-Steady state

Typical steady state drop size distributions as well as steady state cumulative drop size distributions are illustrated in Figures 5 and 6 respectively. These distributions based on more than 1000 drops per distribution are approximately Gaussian as shown in Figure 5. However, the steady state size distribution is slightly skewed towards the smaller drop sizes. This is understandable as only a very small number of drops of size greater than d_{max} can exist at equilibrium. Also due to uniform breakage of droplets over the volume of the reactor, one may expect a broad spectrum of drops less than d_{max} and a comparatively small number of drops of size less than d_{min}. Similar distributions have been reported for kerozene-water

dispersions (Stamatoudis and Tavlarides, 1985) and for a variety of other liquid-liquid systems (Narsimhan et al., 1979) in agitated vessels.

The transient drop size distribution is modelled in section 5.3. It can also be used for determining the steady state drop size distribution, once the time to reach steady state has been identified (Hatzikiriakos et al., 1988**c**).

5.3. Drop Size Distribution-Unsteady state

The design of gas-liquid-liquid tubular reactors requires not only a knowledge of steady state drop size distribution, but also the dynamic characteristics of drop break-up and coalescence. The dynamic character of drop break-up and coalescence has been recognized by various workers (Coulaloglou and Tavlarides, 1977; Shah and Ramkrishna, 1973 and Narsimhan et al., 1980). These workers have approached the problem of prediction of drop size distributions by using population balances. However, such approaches cannot predict breakage and coalescence rates and the dynamic interelationship between them. In this section an attempt is made to characterize the dynamic features of drop breakage in gas-liquid-liquid tubular reactors for lean dispersions. Following Ramkrishna (1973), the probability of drop break-up is quantified and suggestions for evaluating the cumulative drop size distribution function are given. Finally, a comparison between the rate at which steady state drop size distributions are approached in tubular reactors and agitated vessels is performed.

5.3.1. Dynamics of Drop Breakage in Tubular Reactors

The effect of time on drop break-up was studied for lean dispersions (volume fraction=0.0045). Therefore, the effect of drop coalescence may be considered negligible. Three different gas fluxes (u_g=0.1, 0.4 and 2 cm/sec) and three different systems (system B, F and G. Table 1) were chosen. During a typical experiment drop size distributions were obtained after 3, 6,10,15, 30 and 45 minutes. Initially, it was identified that at low gas fluxes steady state was reached in less than 30 minutes. Thus, subsequent drop size distributions were only obtained after 3, 6,10,15 and 30 minutes. In Figures 7, 8 and 9 the cumulative volume distributions of dibenzyl ether, cottonseed oil and linseed oil systems at low, immediate and high gas fluxes respectively are plotted. Time is a parameter. It can be seen that large drops present initially are rapidly broken up and a steady state size distribution profile is obtained in less than 30 minutes. From the same Figures, it may also be observed that as time increases the breadth of drop size distribution narrows and the probability density steepens. Figure 10 shows the impact of superficial gas velocity on the rate at which steady state is reached. For relatively large times (t>3 min) the rates at different gas fluxes are parallel, indicating that no effect exists. Similar observations may be inferred from Figures 11 and 12 where the effects of interfacial tension and relative viscosity are shown. The rates are parallel for times greater than 3 minutes. Therefore, the physical properties of dispersed phase and superficial gas velocities do not have significant effect

on the rate at which steady state is reached. The reduction of mean drop diameter with respect to time for the three systems under investigation is correlated as:

$$d_{vs,t} = d_{vs} (1+1.6\exp(-t/5)) \qquad (5.2)$$

where $d_{vs,t}$ is the mean drop size at time t, d_{vs} is the Sauter mean diameter at steady state and t is time in minutes. Equation 5.2 is represented by the solid line on Figure 17. As it may be seen, it fits the experimental data well. For t=0, the above Equation becomes $d_{vs,t}=2.6d_{vs}$. This suggests that at times less than 3 minutes the rate of break-up may depend on the initial drop size, physical properties of the system and superficial gas velocity. However, for t>3 min a similarity in the rate of drop breakage exists for the systems under investigation.

5.3.2. Similarity and Probability of Drop Breakage

In section 5.3.1 it was concluded that dispersed phase properties and superficial gas velocity do not have a significant effect on the rate at which steady state is reached. This suggests that a similarity in drop breakage should exist with respect to time. In the present section this similarity is identified and subsequently quantified. It is also demonstrated that measurements of cumulative volume distributions of drop sizes at various instants provide all the required information for prediction of unsteady state drop size distributions. The knowledge of drop size distribution at

every instant is of great importance because of the simultaneous nature of drop breakage and transport processes.

If the volume fraction of drops with a volume less than v at time t is denoted by F(v,t) which is a cumulative distribution function, then this function satisfies the following conditions.

$F(v,t)=0$ when $v \leq 0$; $F(v,t)=1$ when $v \rightarrow \infty$

If $\Gamma(v)$ is the transition probability function then $\Gamma(v)\,dt$ represents the probability that a drop of volume v breaks in the time interval (t,t+dt). The volume fraction of daughter drops with volume less than v formed from breakage of a drop of volume v' represented by the function G(v,v'), has the following properties.

$G(v,v')=0$ when $v \leq 0$; $G(v,v')=0$ when $v \geq v'$

Ramkrishna (1973) showed that for a batch operation with lean dispersions, Equation 5.3 can be written,

$$\frac{\partial F}{\partial t} = \int_{F(v,t)}^{F(\infty,t)} \Gamma(v')\, G(v,v')\, dF(v',t) \qquad (5.3)$$

which can be rewritten as

$$\frac{\partial F}{\partial t} = \int_{v}^{\infty} \Gamma(v')\, G(v,v') \frac{\partial F}{\partial v}(v',t)\, dv' \qquad (5.4)$$

where $\partial F/\partial v$ is the density function. At this point $\Gamma(v')$ and $G(v,v')$ must be known functions in order to quantify the cumulative distribution function $F(v,t)$. Ramkrishna (1973) made two assumptions for drop breakage of lean dispersions in agitated vessels. The breakage probability function was assumed to be of the form

$$\Gamma(v) = K\, v^{n} \qquad (5.5)$$

where K and n are constants to be identified from experimental measurements. The function $G(v,v')$ was also assumed to be of the form

$$G(v,v') = g(v/v') \; ; \quad 0 < v/v' < 1 \qquad (5.6)$$

Making use of the Equations 5.5 and 5.6, Equation 5.4 may be rewritten as

$$\frac{\partial F}{\partial t} = \int_{v}^{\infty} K\, v'^{n}\, g(v/v')\, dF(v',t) \qquad (5.7)$$

A similarity variable $z=(1+Kt)v^{n}$ exists for Equation 5.7 (Fillipov, 1961). For times sufficiently large this variable may be simplified to Ktv^{n}. This implies that for a fixed value of $F(v,t)$ (a horizontal line in Figures 7, 8 and 9) the similarity variable $z=Ktv^{n}$ should remain constant if the above postulations are valid.

$Kv^n t=constant$ or $v^n t=constant$

Figures 13 and14 are log-log plots of drop diameter d vs time t for dibenzyl ether and linseed oil systems at superficial gas velocities u_g=0.1 and 2 cm/sec respectively. It can be seen that the slopes of the straight lines are approximately -0.33. This means that the exponent n in Equation 5.5 is approximately 1, because v is proportional to d^3.

Using the approximate value n=1, cumulative distribution functions F(v,t) are plotted against the similarity variable $t^{1/3}d$ for two different systems in Figures 15 and 16. It is shown that the cummulative distributions at various times collapse into a single line. The same behaviour was obtained for all three systems and experimental conditions in this work. Therefore, the existence of the similarity variable in drop breakage of lean dispersions in gas-liquid-liquid tubular reactors has been established. However, it has to be realized that the constant K in Equation 5.5 may be a function of the local intensity of turbulence, operating and design parameters of tubular reactors. Hatzikiriakos et al. (1988**c**) found that K may be related to the stable size spectrum, d_{max}-d_{min}, showing that K is a function of the energy dissipation rate and physical properties of the dispersed phase liquid.

Knowledge of the similarity variable may lead someone in evaluating the density function. However, this is a numerical procedure and out of the scope of the present investigation. Details of the method for determining

the drop size distribution at various instants are given by Ramkrishan (1973).

5.3.3. Comparision with Agitated Vessels (Unsteady state)

Figure 17 is a plot of the ratio $d_{vs,t}/d_{vs}$ against time of column operation. The solid line represents Equation 5.2 and the dashed line represents the rate at which steady state is reached in agitated vessels with lean liquid-liquid dispersions (Narsimhan et al., 1980). The energy dissipation in the agitated vessel corresponds to superficial gas velocity of 4 cm/sec. As it may be concluded from Figure 17, steady state drop size distributions are approached more rapidly in tubular reactors than in agitated vessels.

Ramkrishna (1973) found that the transition probability function $\Gamma(v)$ in agitated vessels with lean dispersions is proportional to d^6. In Section 5.3.2 it was found that $\Gamma(v)$ in tubular reactors with lean liquid-liquid dispersions is proportional to d^3. The large exponent on the drop diameter in the case of agitated vessels indicates that the probability of drop break-up decreases more rapidly than in the case of tubular reactors as the drop size is reduced. This gives a reasonable explanation for why steady state is approached more rapidly in tubular reactors. It also suggests that tubular reactors perform better in the sense that larger interfacial areas are obtained more quickly. However, this is discussed in detail in Section

5.5.

5.4. Maximum, Minimum and Mean Drop Sizes

Maximum, minimum and Sauter mean drop diameters are listed in Table 4 for the bulk of the experiments carried out in this investigation. Maximum and minimum stable drop sizes against break-up and coalescence set limits in the stability of drops in dispersion processes. As a result, a drop with size between these two limits is too small to break up and too large to coalesce. These sizes are also very useful in correlating the mean drop sizes. Sauter mean drop diameter is widely used in estimating the interfacial area. In this subsection the impact of superficial gas velocity and physical properties of dispersed liquid phase on the steady state Sauter mean diameter are discussed and generalized correlations for the maximum, minimum and mean drop sizes are presented. Also a new theory is proposed to account for the functional dependence of maximum and minimum drop sizes on the energy dissipation rates.

5.4.1. Superficial Gas Velocity

5.4.1.1. The Prediction of Mean Drop Size in Tubular Reactors for Gas-Liquid-Liquid Systems

Three flow regimes are clearly identified in the operation of bubble columns for gas-liquid-liquid systems as discussed in section 2.4. In the low gas flux regime, bubbles rise independently and the assumption that

local isotropic turbulence controls break-up is at best approximate. In addition the probability of direct bubble-drop collision is very low as drops tend to follow streamlines around bubbles as they move upwards through the column. The mechanism for drop break-up at low gas fluxes appears to be governed by shear stresses induced by bubble motion, where drop break-up arises from deformation and acceleration (Hatzikiriakos et al., 1988**b**). In APPENDIX B a simple expression is derived giving the maximum stable drop size against break-up as a function of superficial gas velocity in this flow regime:

$$d_{max} \sim \frac{\sigma}{(\mu_c \rho g)^{0.5} f(\mu_d/\mu_c) u_g^{0.5}} \qquad (5.8)$$

The important part of this formula is that maximum drop diameter is expected to change as a function of -0.5 power of superficial gas velocity.

Following the Thomas approach (1980) in APPENDIX C, the minimum stable drop size against coalescence is found to be

$$d_{min} \sim \frac{(\sigma h/\mu_c)^{2/3}(v/g)^{1/6}}{[f(\mu_d/\mu_c)]^{1/3} u_g^{0.5}} \qquad (5.9)$$

in the same flow regime. Again the minimum drop size against coalescence is a function of -0.5 power of superficial gas velocity. In APPENDIX D

arguments originating from a statistical point of view have shown that at low gas rates the superficial gas velocity is almost proportional to terminal velocity of bubbles.

In the high gas flux regime the flow field approaches local isotropic turbulent conditions. In this case Equations 2.9 and 2.10 for the maximum and minimum drop sizes against break-up and coalescence respectively may be applied. In APPENDIX A the energy dissipation in bubble columns has been found to be:

$$\varepsilon = \frac{\Delta\rho \, g \, H \, u_g}{\rho_l H_o} \qquad (5.10)$$

where $\Delta\rho$ is the density difference (continuous phase liquid-gas), ρ_l is the density of the liquid in the reactor, H_o is the initial liquid height and H is the overall pressure drop across the column. Equation 5.10 is based on the assumption that the energy is dissipated uniformly by the liquid in the reactor. The exact proportion absorbed by the dispersed phase cannot be calculated using this relation as a significant fraction of the energy dissipated is absorbed during drop break-up, through the creation of additional interfacial area. If all of the energy is transferred to the dispersed phase, then the power dissipated per unit mass of dispersed phase can be expressed as:

$$\varepsilon = \frac{\Delta\rho\, g\, H\, u_g}{\rho_{ld}\, H_o\, \phi} \qquad (5.11)$$

where ρ_{ld} is the density of the dispersed phase and ϕ is the volume fraction of the dispersed phase. Experimentally one would anticipate that the power dissipated by the dispersed phase would fall between those obtained using Equations 5.10 and 5.11. Applying Equation 2.9, two maximum diameters, $d_{max,d}$ and $d_{min,u}$ can be obtained, where $d_{max,d}$ is the maximum drop size by assuming that the power is dissipated by the dispersed phase exclusively and $d_{max,u}$ is the maximum drop size by assuming that the power is dissipated uniformly by the liquid in the reactor. The maximum stable drop size against break-up would fall between the $d_{max,d}$ and $d_{max,u}$. Using similar arguments and Equation 2.10 two minimum diameters can be obtained, i.e., $d_{min,d}$ and $d_{min,u}$ ($d_{min,d}$ is the minimum stable drop diameter by assuming that the power is dissipated by the dispersed phase exclusively and $d_{min,u}$ is the minimum stable drop diameter by assuming that the power is dissipated uniformly by the liquid in the reactor). Mean drop diameter can be expressed as a function of minimum and maximum diameters obtained from Equations 2.9 and 2.10:

$$d_{vs}=f(d_{min,d},\ d_{min,u},\ d_{max,d},\ d_{max,u}) \qquad (5.12)$$

Postulating similar arguments discussed in Section 2.5 for the effect of relative viscosity μ_d/μ_c, Equation 5.12 may be rewritten as:

$$d_{vs}=f(d_{min,d}, d_{min,u}, d_{max,d}, d_{max,u})(\mu_d/\mu_c)^{0.25} \qquad (5.13)$$

Equation 5.13 is used as a basis for correlating experimental drop size data in this study. The role of dispersed phase volume fraction is not given explicitly in Equation 5.13 since it has been incorporated in the calculation of minimum and maximum drop diameter, based on the assumption that the energy is dissipated by the dispersed phase exclusively.

5.4.1.2. Experimental results

Figure 18 shows the effect of superficial gas velocity on the steady state Sauter mean diameter of dispersed phase liquid drops for the systems used in this investigation. Two flow regimes, one below and one above 0.3 cm/sec are clearly identified by a sharp change in the slope of the functional dependence. For drop break-up to occur, it is necessary that enough energy be supplied to the drop to overcome the forces that resist breakage as a function of interfacial tension. The energy for the drop break-up may be kinetic energy at high gas fluxes (kinetic energy of energy-dissipating eddies), shear energy at low gas fluxes or a combination of the two. As was discussed in section 2.6, dynamic pressure fluctuations are the forces responsible for breakage of drops at high gas fluxes and

shear forces at low gas fluxes. One may expect that two correlations will be derived corresponding to high and low gas fluxes respectively. However, the practical importance of these processes lies at high gas fluxes (Hatzikiriakos et al., 1988a). In addition, most of the experiments carried out in this investigation are related to high superficial gas velocities. Due to these two reasons, an attempt was made to correlate one generalized equation to determine the mean drop size in terms of theoretical minimum and maximum drop sizes:

$$d_{vs}=0.2\ (d_{max,d}+d_{min,d})+0.04\ (d_{max,u}+d_{min,u}) \qquad (5.14)$$

Equation 5.14 fits experimental mean drop diameter within ±30%. This deviation is slightly influenced by the incorporation of mean drop sizes at low gas fluxes. If this correlation for mean drop diameter is modified by including the ratio of dispersed phase viscosity to continuous phase viscosity, it becomes:

$$d_{vs}=(0.201(d_{max,d}+d_{min,d})+(0.0305(d_{max,u}+d_{min,u}))(\mu_d/\mu_c)^{0.256} \qquad (5.15)$$

Equation 5.15 correlates the Sauter mean diameter within ±22%. Close scrutiny of the size distribution data suggested that the effect of interfacial tension on mean drop diameter is overestimated by Equations 2.9 and 2.10 and an additional interfacial tension term is included in the correlation. Sauter mean drop diameter is predicted within ±10% with Equation 5.16:

$$d_{vs}=0.15((d_{max,d}+d_{min,d})+0.7(d_{max,u}+d_{min,u}))\sigma^{-0.52}(\mu_d/\mu_c)^{0.256} \qquad (5.16)$$

where diameters are in microns and σ is interfacial tension in dynes/cm. A parity plot for this correlation is shown in Figure 19. The values calculated from Equation 5.16 are very much comparable to those listed in Table 4.

From Figure 18 it may be seen that the cottonseed and linseed oil systems have identical behaviour and the two flow regimes can be identified clearly. However, the dibenzyl ether system with a relatively low viscosity in comparison with the other two systems under investigation, has the same behaviour at both low and high gas fluxes. This deviation may be attributed to a combined effect of relative viscosity and interfacial tension for systems of low relative viscosity and interfacial tension. Moreover, since the shear stresses are more important at low gas fluxes drop breakage rate depends on the interfacial tension and the shear field outside the drop. As the ratio μ_d/μ_c is closer to unity the shear forces become more effective. Therefore, the Sauter mean diameters for such systems are smaller than expected (a slope -0.5 would give larger drop sizes).

Using the same arguments with those used for correlating the Sauter mean drop diameter, the experimental minimum diameter d_2 (diameter at 2% cummulative volume) and maximum diameter d_{95} (diameter at 95% cummulative volume) were fitted within ±10% using Equations 5.17 and 5.18:

$$d_2=0.314(d_{min,d}+0.7d_{min,u})\sigma^{-0.527}(\mu_d/\mu_c)^{0.256} \qquad (5.17)$$

$$d_{95}=0.523(d_{max,d}+0.7d_{max,u})\sigma^{-0.527}(\mu_d/\mu_c)^{0.256} \quad (5.18)$$

From Equations 5.16, 5.17 and 5.18 it can be observed that $d_{max,d}$, $d_{max,u}$, $d_{min,d}$ and $d_{min,u}$ appear with fixed proportionality constants. This suggests that the energy is dissipated in a fixed proportion by dispersed and continuous liquid phases. The magnitudes of proportionality constants imply that almost 60% of the available energy in the reactor is dissipated exclusively by the dispersed phase. This is understandable and due to the fact that most of the available energy is consumed to increase the interfacial area. However, the fixed percentage (60%) cannot be stated firmly due to the arbitrariness of some parameters e.g., the critical thickness for rupture was taken $h=10^{-5}$ cm, the proportionality constants in Equations 2.9 and 2.10 are not fixed (taking other constants a different percentage would be found). The coefficients of Equations 5.16-5.18 have been obtained through nonlinear least square regression of experimental data. The experimental maximum and minimum diameters have the same functional dependence on energy dissipation rate as mean drop diameter, as shown in Figures 20 and 21 for the cottonseed oil and linseed oil systems respectively. The various slopes related to this functional dependence for both flow regimes, are calculated using least squares and tabulated in Table 5. Therefore, the experimental maxima and minima may be correlated with high accuracy (±1%) as functions of Sauter mean diameters as follows:

$$d_{vs} = 0.5\ d_{95} = 6\ d_2 \quad (5.19)$$

At gas fluxes below 0.3 cm/sec a slope of -0.5 can be noticed for both maximum and minimum diameters. This is in agreement with the slopes predicted by Equations 5.8 and 5.9. However at this point two questions related to the proposed theory have to be discussed before the theory is established. The first question is due to the consideration that drainage takes place between planes steadily pressed together for a period determined by the lifetime, T, of maximum shear stress (the equator of a bubble where the stresses are concentrated, needs time equal to $T=d_p/U_T$ in order to pass by a drop). One may wish to know, if the characteristic time for two colliding drops t_o, known as natural rebound time, is less than the characteristic time T defined in APPENDIX C for a two droplet encounter. If one pressumed that T is always less than t_o, then coalescence would always happen even if shear stresses are no longer configured. The characteristic time t_o is given by Lamb (1945) as:

$$t_o = (\rho_d d_p^3/\sigma)^{1/2} \qquad (5.20)$$

Taking the ratio t_o/T using Equations 5.20 and $T \sim d_p/U_T$,

$$t_o/T = U_T(\rho_d d_p/\sigma)^{1/2} \qquad (5.21)$$

This ratio in all cases under investigation is less than unity, giving an answer to one's concern about the duration problem For example, taking the surface tension to vary from 5 to 26 dynes/cm, d_p from 20 to 100 μm and

U_T from 15 to 30 cm/sec, which includes all the cases under investigation, the ratio t_o/T is always less than unity.

The second question arises from the following argument. Since the model assumes that the droplets are pressed together by a steady force and that the film is drained between plane solid surfaces, the predicted d_{min} sizes should be smaller than the boundary layer thickness in the surroundings of the bubbles. For example, taking the size of the bubbles to vary from 1.3 to 2.2 cm (typical sizes encountered in the present work), the boundary layer thickness may be easily calculated to be in the range 230-260 μm. Experimental minimum drop sizes are in the range 25-90 μm. Additionally, by applying Equation C.6 for some typical values of σ, μ_c, $h=10^{-5}$ cm and U_T (f(p) may be neglected, since in Taylor's expression changes a little for $5<p<19$ $f(p)=(19p+16)/(16p+16)$), minimum drop sizes are calculated to be in the range 25-65 μm. Therefore, these results justify the assumptions made for the present model. However, it has to be kept in mind that this theory is valid only for inviscid continuous phase and need to be modified for a more viscous continuous phase.

At high gas fluxes a slope of -0.25 is obtained for both maximum and minimum drop diameters. The -0.25 power law dependence of minimum drop diameter conforms with Equation 2.10 derived by Thomas (1981). However, one would expect a -0.4 power law dependence of maximum drop diameter on the rate of energy dissipation. This deviation may be attributed to the

following reasons:

-The Equations 2.9 and 2.10 have been derived under the assumption of isotropic turbulent conditions. The energy-dissipating eddies are responsible for break-up and coalescence of drops in isotropic turbulent flows. The length and velocity scales of these eddies are very much comparable with the minimum drop sizes. At these microscales, isotropic turbulent conditions may be reasonably considered. However, due to an order of magnitude difference in size between maximum and minimum drop diameters, isotropic turbulent conditions may not be considered at scales comparable to maximum drop sizes.

-The axial dispersion coefficient considerably exceeds the radial dispersion coefficient in tubular reactors (Reith et al., 1968). This finding is not consistent with conditions prevalent in isotropic turbulent fields.

-Zakrewski (1981) measured the intensity of turbulence in bubble columns and found that the spectral energy distribution follows a k^{-2} law instead of $k^{-5/3}$ law predicted from Kolmogoroff theory, where k is the wave number. In spite of this deviation from theory, Equations 5.17 and 5.18 predict the maximum and minimum drop sizes reasonably well by including the additional correction term of interfacial tension. This correlation derived under the consideration of isotropic turbulent conditions is very simple and appears to be applicable to a wide range of operating conditions.

Steady state drop size distribution as well as mean drop diameters are affected by changes in superficial gas velocity, as shown in Figures 22 and

23. The range of stable drop sizes narrows as the superficial gas velocity is increased. This has also been found by Shinnar (1961). As the energy dissipation rate increases and the maximum and minimum drop sizes become even more comparable in size, a dynamic equilibrium between coalescence and break-up occurs. A similar dependence is noted for agitated vessels (Stamatoudis and Tavlarides, 1985). The distributions of the number of drops over the drop size spectrum have a similar dependence on the energy dissipation rate as may be noticed from Figures 24 and 25. These distributions are not Gaussian but are severely skewed towards the smaller sizes. As the rate of energy dissipation increases, the number of smaller drops increases dramatically. The probability density becomes steeper in the smaller sizes due to the number of drops in this part of the drop size spectrum.

5.4.2. Viscosity

The impact of relative viscosity on the Sauter mean diameter is illustrated in Figure 26. The various systems used for sketching this Figure have almost the same interfacial tension (6.1-6.8 dynes/cm). Superficial gas velocity is a parameter. The slope of the curves are related to the power dependence of Sauter mean diameter on relative viscosity, μ_d/μ_c. A power dependence of 0.256 was obtained by nonlinear regression on the experimental data which conforms with the value, 0.25, obtained by Calderbank (1967) for bubbles in agitated vessels. Such a dependence may

also apply to steady state Sauter mean diameter of bubbles in bubble columns under certain operating conditions (Shah et al., 1982). Nishikawa et al. (1987) reported a power dependence ranging from 0.125 to 0.2 for liquid-liquid systems in agitated vessels.

As it is seen from Figure 26, the dependence of the steady state Sauter mean diameter seems to be the same at both low and high gas fluxes. The existence of different mechanisms of drop splitting at different flow regimes does not appear to affect this dependence. Using least squares on each line appearing on Figure 26, various slopes were calculated with a standard deviation of 5%. At low gas fluxes where shear forces dominate, the ratio of drop viscosity to that of the suspending fluid is an important dimensionless group in governing drop deformation and burst (Rallison, 1984). This group plays the role of matching the normal and tangential stresses at the liquid-liquid interface. As this ratio deviates from the range of 0.1 to 1 to either higher or lower values, drop resistance to break-up becomes greater and greater. These theoretical arguments conform with studies on dispersion phenomena at simple flows like couette and hyperbolic flows (Grace, 1982) and at those of the present work. At high gas fluxes where dynamic pressure fluctuations dominate, the dependence of the steady state Sauter mean diameter on relative viscosity is also consistent with theory (Hinze, 1955). There is no experimental evidence related to the dependence of Sauter mean diameter on relative viscosity for gas-liquid-liquid systems in tubular reactors.

It has to be pointed out that at high gas fluxes and for the dibenzyl ether system (low interfacial tension and viscosity) a milky emulsion is formed. Photographs could not be taken. However, an expected Sauter mean diameter is close to 100 μm, as may be seen from the extrapolated line in Figure 26.

The role of viscosity is not limited to the ratio of drop viscosity to that of the suspending fluid. The viscosity of continuous phase itself is also of great importance. The time τ required for the film of a two-drop encounter to drain to the critical rupture thickness h decreases as the viscosity of continuous phase decreases. In such a case, the rate of drop coalescence increases, as a result, bigger drops may be observed (Stamatoudis and Tavlarides, 1985).

5.4.3. Interfacial Tension

Interfacial tension has a limited influence on mean drop diameter as shown in Figure 18. The systems cottonseed oil and linseed oil, for examble, have approximately the same viscosity but different interfacial tensions. The effect of interfacial tension on mean drop size is less than anticipated by the Equations of Thomas and Hinze which are based on isotropic turbulence. This difference may be attributed to the efficiency and modes of energy transfer to the dispersed phase which may not conform with conditions prevalent in isotropically turbulent flow fields. This was discussed in Section 5.4.1.b and it was concluded that isotropic turbulent conditions are not consistent with conditions prevalent in bubble columns

at least in length scales comparable to maximum stable drop sizes against break-up. Equation 5.15 based on isotropic turbulence conditions fits the experimental Sauter mean drop diameters within ±22%. Once the additional term of interfacial tension σ is included, Equation 5.16 predicts Sauter mean diameter within ±10%.

From Table 4, it may be seen that the effect of interfacial tension on Sauter mean diameter as well as on maximum and minimum drop diameters is stronger at low gas fluxes than at high gas fluxes. The differences in d_{vs}, d_{max} and d_{min} for the systems cottonseed oil and linseed oil, for example are comparatively larger at low gas fluxes. This is understandable if one takes into consideration that at low gas fluxes the interfacial tension forces oppose the shear forces in deforming the drops. Therefore a conflict between shear forces and interfacial tension forces exist and the drop breakage is expected to depend on the surface tension and on the hydrodynamic field outside the drop. At high gas fluxes, one has to consider the problem from an energy point of view. The deformation and bursting of drops are continuous processes since the drops are under the action of dynamic pressure fluctuations at every instant. Therefore, drops may promote larger deformations. For highly deformed drops, interfacial tension is in favor with splitting instead of resisting to it (Rallison, 1984). Since there is no limitation in energy, the assumption of the existence of highly deformed drops in turbulent fields is reasonable. The impact of interfacial

tension is also discussed below in section 5.5, where the tubular reactors are compared with the agitated vessels.

5.4.4. Dispersed Phase Concentration

The effect of dispersed phase concentration on Sauter mean diameter is shown in Figures 27 and 28 for linseed oil and cottonseed oil systems respectively. The solid lines on these Figures represent Equation 5.16. It may be seen that this corelation can predict the effect of dispersed phase concentration very well. It is also shown that Sauter mean diameter increases with the dispersed phase concentration. This dependence is expected to be stronger for denser dispersions ($\phi > 0.10$) since the coalescence rate of drops increases with concentration (Mlynek and Resnick, 1972; Coulaloglou and Tavlarides, 1976). However, for lean dispersions ($\phi < 0.0045$), it was found that the dispersed phase concentration had no effect on Sauter mean diameter. A similar behavior is noted for agitated vessels (Narsimhan et al., 1976). A limited dependence on concentration has also been reported by Nishikawa et al. (1987) for dense liquid-liquid dispersion in agitated vessels. Kato et al. (1984) reported that at $\phi > 0.05$ concentration had little impact on Sauter mean diameter in gas-liquid-liquid bubble columns.

From Figures 27 and 28, it may also be inferred that the impact of volume fraction of dispersed phase on Sauter mean diameter is the same at both low and high gas fluxes. The role of dispersed phase concentration is

not given explicitly in Equation 5.16 since it has been incorporated in the calculation of minimum and maximum drop diameters based on the assumption that the energy is dissipated by the dispersed phase exclusively.

5.4.5. Density

The relative density of the dispersed and continuous phases, ρ_{ld}/ρ_{lc}, had no effect on Sauter mean diameter in the range $0.95 < \rho_{ld}/\rho_{lc} < 1.05$. In Table 6, the Sauter mean diameters for three subsets of experiments are listed. In each subset the superficial gas velocity and interfacial tension are kept constant. The differences in d_{vs} may be attributed to relative viscosity which has a significant effect on d_{vs} as it is discussed in Section 5.4.2. Therefore, the Sauter mean diameters have to be corrected using Equation 5.16 in order to account for the different relative viscosities. In Table 6, the corrected Sauter mean diameters are listed in contrast with the real Sauter mean diameters. Basis is taken as $\mu_d/\mu_c=13$, an intermediate value. As it may be observed, the differences for the first subset of experiments are very small and these can be attributed to experimental error or the effect of interfacial tension. However, the data for the other two subsets of experiments is inconclusive.

Hinze (1955) concluding his clasical paper pointed out that the difference in density between the dispersed and the continuous phases has an important effect on the way in which break-up occurs. Thus, it has to be

realized that correlations for Sauter mean diameters using the maximum and minimum drop diameters should be based on data without a basic difference in densities between the two phases. If there is, incorrect results might be obtained. This turns out not to be the case, only if the role of relative density has to be assessed independently. Following these concluding remarks of Hinze, data with difference in the density of the two liquid phases are not included in the correlations 5.16-5.18.

5.4.6. Other Parameters

The initial drop size has no effect on the steady state Sauter mean diameter for initial drop sizes in the range 2000μm<d<10000μm. However, the initial drop size have an impact on the drop breakage rate for times less than about 3 min, as it is discussed in Section 5.3.1.

Operating the column under constant pressure, constant gas rate or intermediate conditions, different bubble sizes are obtained at constant gas fluxes. It was found that bubble sizes in the range 10 to 25 mm had no apparent effect on mean drop diameter. However, it has to be emphasized that at high gas fluxes, the photographic technique used in this investigation is limited to the bubbles in the vicinity of the column wall. At these high gas fluxes, the large bubbles tend to rise in the central plume of the column. Therefore, the upper limit of 25 mm is a little higher in reality.

A perforated plate was placed 5 cm above the nozzles in order to avoid

drop break-up because of the air jet, in particular at high gas fluxes. However, such an effect was not observed and the rest of the experiments were performed following the procedure described in Section 3.2.

Finally, a perforated plate was placed 5 cm below the free surface of continuous liquid phase in order to avoid free surface effects on drop break-up, which might have an impact on the Sauter mean diameter.

5.5. Comparison with Agitated Vessels (Steady State)

Agitated vessels are widely used in Chemical Engineering as contactors for liquid-liquid systems because of their effectiveness in bringing about the contact of two liquid phases. Their characteristics are discussed in Section 2.5. On the other hand, bubble columns are also used extensively for gas-liquid systems because of low investment costs and effective mixing of fluids. Their characteristics are presented in Section 2.3.

In this section an attempt is made to compare the relative performance of tubular reactors and agitated vessels as contactors for liquid-liquid systems. This comparison is based on the energy consumption per unit of interfacial area. In particular, the results of this investigation are compared with those of Nishikawa et al. (1987), who summarized the impact of operating parameters and physical properties of both liquid phases on the Sauter mean diameter of dispersed phase drops in agitated vessels operating at steady state with Equations 2.13 and 2.14 given in section 2.5.

The impact of power dissipation on the Sauter mean diameter for

agitated vessels and tubular reactors is illustrated for three different systems in Figure 29. For linseed oil system, Figure 29.a, a system with high viscosity and low interfacial area, the mean diameters $d_{vs.a}$ and $d_{vs.b}$ obtained in an agitated vessel and a tubular reactor respectively are comparable. The ratio $d_{vs.a}/d_{vs.b}$ converges at high energy dissipation rates. The large mean diameters obtained at low energy dissipation rates in agitated vessels can be attributed to coalescence in zones remote from the impeller (Mlynek and Resnick, 1972; Weinstein and Treybal, 1973).

Figure 29.b shows the effect of energy dissipation rate on Sauter mean diameter for the cottonseed oil system, a system with high viscosity and high interfacial tension. It can be observed that mean drop diameter is much greater in agitated vessels as far as liquid-liquid systems are concerned. This may be attributed to the local energy dissipation and accordingly to the intensity of turbulence which is more uniform in the tubular reactors. In the agitated vessels, the Sauter mean diameter might be affected significantly by the local intensity of turbulence in the vicinity of the impeller. The zones remote from the impeller in the tank remain less effective for liquid-liquid systems. To gain a better understanding of this fact, it has to be realized that the drop deformation and breakage are time-dependent processes. In agitated vessels the drops circulate from zones of high energy dissipation to zones of low energy dissipation. Therefore, there may not be enough time in order for the drops to be

deformed critically. On the other hand in tubular reactors the drops are under the action of dynamic pressure fluctuations for longer times. Therefore, the required energy for drop bursting is accumulated easier. Yoshida and Yamada (1972) performed experiments in both tubular reactors and agitated vessels for dispersion of kerozene in water. This system has high interfacial tension (43 dynes/cm) and low viscosity (1.29 cp). It was found that the Sauter mean diameter of kerozene droplets in the tubular reactor was approximately one half of that in the agitated vessel. These findings are consistent with those of the present work.

Figure 29.c shows the same comparison for the dibenzyl ether system, a system with low viscosity and interfacial tension. In this case, agitated vessels and tubular reactors perform equally well. Clearly, the comparative advantage for tubular reactors is greatest for fluids with high interfacial tension as the steady state Sauter mean diameter has only a limited dependence on interfacial tension in these reactors.

6.0. CONCLUSIONS

A number of characteristics related to gas-liquid-liquid systems in tubular reactors were investigated. Tubular reactors were compared with liquid-liquid agitated vessels on the basis of their relative performance as phase-contacting equipment. The results of this investigation may be summarized as:

1. Gas Flux: as it was expected the gas flux plays an important role in determining the steady state Sauter mean diameter of dispersed phase drops. It was found that Sauter mean diameter is decreased more significantly with gas flux at low gas rates. Two flow regimes, one below and one above ~ 0.3 cm/sec, were identified on a plot d_{vs} vs ϵ by a sharp change in the slope of the functional dependence.

2. Physical Properties of Dispersed Phase Liquid: the physical properties of dispersed phase constituents have a significant impact on the steady state drop size and drop size distribution. Generally steady state Sauter mean diameter increases strongly with relative viscosity, moderately with dispersed phase volume fraction and slightly with interfacial tension. The relative density was not found to have an effect in the range 0.95 to 1.05 $g.cm^{-3}$. The steady state Sauter mean diameter was correlated as a function of gas flux and physical properties of dispersed phase liquid. This correlation predicts mean drop sizes within ±10%.

3. Maximum and Minimum Stable Drop Sizes: a new theory was proposed to

explain the functional dependence of maximum and minimum stable drop sizes against break-up and coalescence respectively at low gas rates on the energy dissipation rate. Two formulae were derived corresponding to maximum and minimum stable drop sizes which give an approximation of the order of magnitude of these sizes at low gas fluxes. At high gas fluxes the functional dependence was attempted to be explained with the isotropic turbulence theory of Kolmogoroff. However, it was found that bubble columns are not quite isotropic even at microscales comparable to maximum drop sizes (500 μm).

4. Unsteady State Drop Size Distribution: the rate at which steady state is reached was found to be independent of the superficial gas velocity and the physical properties of the dispersed phase liquid. The reduction in mean drop size was correlated as a function of time. The existence of a similarity variable was identified and suggestions were made for modeling the unsteady state drop size distribution as a function of time. The transition probability function was found to be proportional to drop volume v in contrast with v^2 in the agitated vessels.

5. Comparision with Agitated Vessels: as mean drop diameter is less dependent on interfacial tension in tubular reactors than in agitated vessels, the comparative advantage is greatest for two phase liquids with high interfacial tensions. Tubular reactors are also preferred for two phase liquids with a high relative viscosity, at low energy dissipation rates. A comparision between tubular reactors and agitated vessels operating under

unsteady state conditions showed that tubular reactors can perform better for all liquid-liquid systems. This is attributed to different functional dependence of the transition probability function on the droplet volume in tubular reactors and agitated vessels.

7.0. RECOMMENDATIONS

The results of this investigation suggest that studies to the following areas are warranted:

1. The isotropic turbulent theory of Kolmogoroff generally gives simple models, applicable to a wide range of operating conditions. However, this theory is sometimes hidden by empiricism. The efficiency and modes of energy dissipation have to be investigated further, particularly in tubular reactors where it was found that these reactors are not quite isotropic even at scales comparable to maximum drop sizes (500 μm).

2. The continuous phase viscosity μ_c itself is expected to have a strong impact on the steady state mean drop size. As μ_c increases, bubbles slow down and the required time τ for the film in a two-drop encounter to drain to the rupture thickness h increases. Therefore, coalescence rates will be important only at high volume fractions of dispersed phase.

3. In lean liquid-liquid dispersions, the effect of drop coalescence is negligible. Therefore, to model the transient droplet breakage only the effect of break-up has to be considered. However, in dense liquid-liquid dispersions population balances have to include the effect of coalescence as well. Dynamic relationships between break-up and coalescence have to be found and checked with experimental data.

4. Interfacial area has a direct impact on mass transfer processes. Gas-liquid and liquid-liquid interfacial areas are expected to play a role for

mass transfer from the gas phase to dispersed liquid phase. The mechanism or the mechanisms of mass transfer in G-L-L systems should be studied.

5. Gas-bubble plate interactions in multi-stage tubular reactors are expected to improve mass transfer rates and impose local axial mixing patterns for the liquid phase above and below the plate. However, the existence of plates may impose milder conditions than those without plates as far as the gas flux remains the same. This may lead to a decrease in interfacial area or an increase in gas requirements. All these effects have to be quantified in terms of process variables in order to be applied to the design of a novel tubular reactor.

8.0. NOTATION

A	cross sectional area of tubular reactor
Bo	bubble Bond number,=$\rho_g g\alpha^2/\sigma_{g\text{-}l}$
C	proportionality constant in Equation 2.11
d	diameter of impeller in Equations 2.13 and 2.14
d_p	drop diameter, μm
d_{vs}	Sauter mean drop/bubble diameter, μm
$d_{vs.a}$	Sauter mean diameter (agitated vessel), μm
$d_{vs.b}$	Sauter mean diameter (tubular reactor), μm
$d_{vs,t}$	Sauter mean diameter at time t, μm
d_{min}	minimum stable drop size, μm
d_{max}	maximum stable drop size, μm
$d_{min,u}$	minimum drop diameter (uniform energy dissipation), μm
$d_{min,d}$	minimum drop diameter (assuming all energy is dissipated to the dispersed phase), μm
$d_{max,u}$	maximum drop diameter (uniform energy dissipation), μm
$d_{max,d}$	maximum drop diameter (assuming all energy is dissipated to the dispersed phase), μm
d_2	experimental minimum diameter at 2% cummulative vol.%, μm
d_{95}	experimental maximum diameter at 95% cummulative vol.%, μm
d_b	diameter of a spherical bubble, cm
d_e	equivalent diameter of a bubble, cm
D	diameter of impeller in agitated vessels, cm; diameter of agitated vessel in Equations 2.13 and 2.14, cm
D_o	diameter of the orifice, cm
f(p)	function of relative viscosity
F(v,t)	volume fraction cumulative distribution function of drop size
Fr	bubble Froud number, $Fr=U_T(\rho_l/(\Delta\rho g d_b))^{0.5}$
F	force, dynes
g	gravitational accelaration constant, $cm.s^{-2}$
G	shear rate, s^{-1}
G(v,v')	cummulative distribution function of daughter droplet size from break-up of a large drop
h	critical rupture thickness, $\sim 10^{-5}$ cm
H	liquid depth, cm

H_o	initial liquid depth, cm
k	wave number, $k=2\pi/\lambda$, cm^{-1}
K	constant in Equation 5.6
n	constant in Equation 5.6
N	number of revolutions of impeller per unit time in Equation 2.11; number of bubbles rising per unit time
N_c	dimensionless capacitance number
N_w	dimensionless number, $N_w=Bo\ Fr^{.5}$
p	relative viscosity of continuous liquid phase to dispersed liquid phase, $p=\mu_d/\mu_c$
P	pressure, cm of continuous liquid phase
P_h	hydrostatic pressure at orifice plate, cm of continuous liquid phase
Re	bubble Reynolss number, $Re=U_T d_e \rho_l/\mu_c$
s	film radious in a two-drop encounter, cm
t	time, min
t_o	natural rebound time of a drop, s
T	characteristic time scale, s
u	velocity scale of energy-dissipating eddies, cm.s
u_s	slip velocity of a bubble swarm, cm.s
u_g	superficial gas velocity, cm.s
U_T	terminal velocity of bubble, cm.s
v	drop volume, cm^{-3}
v'	drop volume, cm^{-3}
V_c	volume of the chamber, cm^{-3}
z	similarity variable,$=Ktv^n$

GREEK LETTERS

α	equivalent radius of bubble, cm
$\Gamma(v)$	transition probability function characterizing droplet breakage
$\Delta\rho$	difference in density between continuous phase liquid and gas, $g.cm^{-3}$
ε	energy dissipation per unit mass, $cm^2.s^{-3}$
ε_d	energy dissipation per unit mass of dispersed phase liquid, $cm^2.s^{-3}$
ε_o	critical energy dissipation per unit mass, $cm^2.s^{-3}$
ε_g	gas holdup

η	length scale of energy dissipating eddies, cm
θ_w	the wake angle behind a bubble
λ	wavelength, cm
μ_c	viscosity of continuous phase, $g.cm^{-1}.s^{-1}$
μ_c	viscosity of dispersed phase, $g.cm^{-1}.s^{-1}$
ν	kinematic viscosity of continuous phase liquid, $cm^2.s^{-1}$
ρ_l	density of the continuous phase liquid, $g.cm^{-3}$
ρ_{ld}	density of dispersed phase liquid, $g.cm^{-3}$
ρ_g	density of gas, $g.cm^{-3}$
σ	interfacial tension, dynes/cm
σ_{g-l}	gas-liquid surface tension, dynes/cm
τ	time required for the film to drain to thickness h, s
ϕ	volume fraction of dispersed phase liquid

9.0. REFERENCES

Abou-El-Hassan, M.E., "Mixing and Phase Distribution in Two and Three Phase Bubble Column Reactors," *3rd European Conference on* **MIXING,** 303 (1979).

Akita, K. and F. Yoshida, "Gas Holdup and Volumetric Mass Transfer Coefficient in Bubble Columns," *Ind. Eng. Chem. Proc. Des. Dev.,* **12,** 76 (1973).

Akita, K. and F. Yoshida, "Bubble Size, Interfacial Area and Liquid Phase Mass Transfer Coefficients in Bubble Columns, " *Ind. Eng. Chem. Proc. Des. Dev.,* **13,** 84 (1974).

Batchelor, G.K., "The Theory of Homogeneous Turbulence," Cambridge University Press (1960).

Begovich, J.M. and J.S. Watson, "Hydrodynamic Characteristics of Three Phase Fluidized Beds," *Fluidization,* Proc. 2nd Eng. Found. Conf., ed., J.F. Davidson and D.L. Keairns, 190 (1978).

Burckhart, R., and W.D. Deckwer, "Bubble Size Distribution and Interfacial Areas of Electrolyte Solutions in Bubble Columns," *Chem. Eng. Sci.,* **30,** 351 (1975).

Calderbank, P.H., "Gas Absorption from Bubbles," *The Chem. Engr.,* **45,** CE209 (1967).

Clift, R., J.R. Grace and M.E. Weber, "Bubbles, Drops and Particles," Academic Press, New York, San Francisco and London (1978).

Coulaloglou, C.A. and L.L. Tavlarides, "Drop Size Distributions and Coalescence Frequencies of Liquid-Liquid Dispersion in Flow Vessels," *A.I.Ch.E. J.,* **22,** 289 (1976).

Coulaloglou, C.A. and L.L. Tavlarides, "Description of Interaction Processes in Agitated Liquid-Liquid Dispersions," *Chem. Eng. Sci.,* **32,** 1289 (1977).

Davidson, J.F. and B.O.G. Schuler, "Bubble Formation at an Orifice in an Inviscid Liquid," *Trans. Instn. Chem. Engrs.,* **38,** 335 (1960).

Davidson, J.F. and B.O.G. Schuler, "Bubble Formation at an Orifice in a Viscous Liquid," *Trans. Instn. Chem. Engrs.,* **38,** 144 (1960).

Davies, R.M. and Sir G.I. Taylor, "The Mechanism of Large Bubbles Rising through Liquids in Tubes," *Proc. Roy. Soc., Ser* **A200,** 375 (1950).

Fillipov, A.F., "On the Distribution of the Sizes of Particles which Undergo Splitting," *Theory Prob. Applic.,* **6,** 275 (1961).

Grace, J.R., T. Wairegi and T.H. Nguyen, "Shapes and Velocities of Single Drops and Bubbles Moving Freely through Immiscible Liquids," *Trans. Inst. Chem. Eng.,* **54,** 167 (1976).

Grace, J.R., "Dispersion Phenomena in High Viscosity Immiscible Fluid Systems and Application of Static Mixers as Dispersion Devices in such Systems," *Chem. Eng. Commun.,* **14,** 225 (1982).

Guthrie, R.I.L. and A.V. Bradshaw, "Behavior of Large Bubbles Rising through Molten Silver," *Chem. Eng. Sci.,* **24,** 913 (1969).

Hadamard, J.S., "Mouvement Permanent lent d'une Sphere Liquide dans un Liquide Visqueux," *C.R. Acad. Sci.,***152,** 1735 (1911).

Hatate, Y., S. Mori, S. Okuma and Y. Kato, "Drop Size in Gas-Liquid-Liquid System Bubble Columns," *Kagaku Kogaku Ronbunshu,* **2,** 133 (1976).

Hatzikiriakos, S.G., R.P. Gaikwad and J.M. Shaw, "Characterization of Gas-Liquid-Liquid Tubular Reactors," Submitted to *A.I.Ch.E. J.* (1988**a**).

Hatzikiriakos, S.G., R.P. Gaikwad and J.M. Shaw, "Drop Break-up and Coalescence in Gas-Liquid-Liquid Tubular Reactors," In Preparation (1988**b**).

Hatzikiriakos, S.G., R.P. Gaikwad and J.M. Shaw, "Transient Drop Size Distribution in Gas-Liquid-Liquid Tubular Reactors," In Preparation (1988**c**).

Hikita, H., S. Asai, K. Tanigaga, K. Segawa and M. Kitao, "Gas Holdup in Bubble Column," *Chem. Eng. J.,* **20,** 59 (1980).

Hinze, J.O., "Fundamentals of the Hydrodynamic Mechanism of Splitting in Dispersion Processes," *A.I.Ch.E. J.,* **1,** 289 (1955).

Hughes, R.B., A.E. Handlos, H.D. Evans and R.L. Maycock, "Formation of Bubbles at Simple Orifices," *Chem. Eng. Progr.,* **51,** 557 (1955).

Hughmark, G.A., "Holdup and Mass Transfer in Bubble Columns," *Ind. Eng. Chem. Proc. Des. Dev.,* **6,** 218 (1967).

Kato, Y., A. Nishiwaki, F. Takashi and S. Tanaka, "The Behavior of Suspended Particles and Liquid in Bubble Columns," *J. Chem. Eng. Japan,* **5,** 112 (1972).

Kato, Y., A. Nishiwaki, S. Tanaka and T. Fukuda, "Longitudinal Concentration Distribution of Suspended Solid Particles in Multi-stage Bubble Columns," *J. Chem. Eng. Japan,* **15,** 376 (1982).

Kato, Y., T. Kago and S. Morooka, "Longitudanal Concentration Distribution Droplets in Multi-stage Bubble Columns for Gas-Liquid-Liquid Systems," *J. Chem. Eng. Japan,* **17,** 429 (1984).

Kito, M., M. Shimida, T. Sakai, S. Sugiyama and C.Y. Wen, "Performance of Turbulent Bed Contactor, Gas Holdup and Interfacial Area under Liquid Stagnant Flow," *Fluidization,* 411 (1976).

Kolmogoroff, A.N., "The Local Structure of Turbulence in Incompressible Viscous Fluid for Very Large Reynolds Numbers," *C.R. Acad. Sci. U.S.S.R.,* **30,** 301 (1941).

Kolmogoroff, A.N., "On the Disintegration of Drops in Turbulent Flow," *Doklady Akad. Nauk. U.S.S.R.,* **66,** 825 (1949).

Kumar, A., T.T. Dagaleesan, G.C. Laddha and H.E. Hoelscher, "Bubble Swarm Characteristics in Bubble Columns," *Can. J. Chem. Eng.,* **54,** 503 (1976).

Kumar, R. and N.R. Kuloor, "The Formation of Bubbles and Drops," *Adv. Chem. Eng.,* **8,** 256 (1970).

La Nauze, R.D. and I.J. Harris, "On a Model for the Formation of Gas Bubbles at a Single Submerged Orifice under Constant Pressure Conditions," *Chem. Eng. Sci.,* **27,** 2102 (1972).

La Nauze, R.D. and I.J. Harris, "A Note on the Gas Bubble Formation Models," *Chem. Eng. Sci.,* **29,** 1663 (1973).

Lane, W.R. and H.L. Green, "Surveys in Mechanics" (G.K. Batchelor and R.M. Davies, eds.), 162, Cambridge Univ. Press, London and N w Yrrk (1956).

Marmur, A. and E. Rubin, "Equilibrium Shapes and Quasi-Static Formation of Bubbles at Submerged Orifices," *Chem. Eng. Sci.,* **28,** 1455 (1973).

Marmur, A. and E. Rubin, "A Theoretical Model for Bubble Formation at an Orifice Submerged in an Inviscid Liquid," *Chem. Eng. Sci.,* **31,** 453 (1976).

Maruayama, T., S. Yoshida and T. Mizushina, "The Flow Transition in a Bubble Column," *J. Chem. Eng. Japan,* **14,** 352 (1981).

McCann, D.J. and R.G.H. Prince, "Bubble Formation and Weeping at a Submerged Orifice," *Chem. Eng. Sci.,* **24,** 801 (1969).

Meister, B. and G.F. Scheele, "General Stability Criteria," *A.I.Ch.E. J.,* **13,** 682 (1967).

Mlynek, Y. and W. Resnick, "Drop Sizes in an Agitated Liquid-Liquid System," *A.I.Ch.E. J.,* **18,** 290 (1972).

Molerus, O. and M. Kurtin, "Hydrodynamics of Bubble Columns in the Uniform Bubbling Regime," *Chem. Eng. Sci.,* **40,** 642 (1985).

Moore, D.W., "The Boundary Layer on a Spherical Gas Bubble," *J. Fluid Mech.,* **16,** 161 (1962).

Moore, D.W., "The Velocity of Rise of Distorted Gas Bubbles in a Liquid of Small Viscosity," *J. Fluid Mech.,* **23,** 749 (1965).

Mugele, R.A. and H.D. Evans, "Droplet Size Distribution in Sprays," *Ind. Eng. Chem.,* **43,** 1317 (1951).

Nakamura, M., K. Hioki, A. Takahashi, H. Tanahashi and S. Watari, "Fluid Flow Characteristics of the Three Phase Fluidized Bed with Perforated Plates," *Kagaku Kogaku Ronbunshu,* **5,** 473 (1978).

Narsimhan G. and J.P. Gupta, "A model for Transitional Breakage Probability of Droplets in Agitated Lean Liquid-Liquid Dispersions," *Chem. Eng. Sci.,* **34,** 257 (1979).

Narsimhan, G., D. Ramkrishna and J.P. Gupta, "Analysis of Drop Size Distributions in Lean Liquid-Liquid Dispersions," *A.I.Ch.E. J.,* **26,** 991 (1980).

Nishikawa, M., F. Mori and S. Fujieda, "Average Drop Size in a Liquid-Liquid Phas Mixing Vessel," *J. Chem. Eng. Japan,* **20,** 82 (1987).

Rallison, J.M., "The Deformation of Small Viscous Drops and Bubbles in Shear Flows," *Ann. Rev. Fluid Mech.,* **16,** 45 (1984).

Ramakrishnan, S., R Kumar and N.B. Kuloor, "Studies in the Bubble Formation-I, Bubble Formation under Constant Flow Conditions," *Chem. Eng. Sci.,* **24,** 731 (1968).

Ramkrishna, D., "Drop-Breakage in Agitated Liquid-Liquid Dispersions," *Chem. Eng. Sci.,* **29,** 987 (1974).

Reith, T., S. Renken and B.A. Israel, "Gas Holdup and Axial Mixing in the Fluid Phase of Bubble Columns," *Chem. Eng. Sci.,* **23,** 619 (1968).

Ruff, K., "Formation of Gas Bubbles at Nozzles during Constant Volume Throughout," *Chem. Ing. Tech.,* **44,** 1360 (1972).

Rybczynski, W., "Uber Die Fotsschreitende Bewegung Einer Flussigen Kugel in Einem Zahen Medium," *Bull. Int. Acad. Pol. Sci. Lett., Cl. Sci. Math. Nat., Ser.A* **40** (1911).

Satyanarayan, A., R. Kumar and N.R. Kuloor, "Studies in Bubble Formation-II, Bubble Formation under Constant Pressure Conditions," *Chem. Eng. Sci.,* **24,** 749 (1968).

Schugerl, K., J. Lucke and U. Oels, "Bubble Columns Bioreactors," *Adv. Biochem. Eng.,* **7,** 1 (1977).

Shah, Y.T., B.G. Kelkar and S.P. Godbole, "Design Parameter Estimations for Bubble Column Reactors," *A.I.Ch.E. J.,* **28,** 353 (1982).

Shah, B.H. and D. Ramkrishna, "Population Balance Model for the Mass Transfer in Lean Liquid-Liquid Dispersions," *Chem. Eng. Sci.,* **28,** 389 (1973).

Shaw, J.M., "Novel Design Criteria for Direct Coal Liquefaction Reactors," Ph. D. Thesis, University of British Columbia (1985).

Shaw, J.M., R. Gaikwad and D.A. Stowe, "Phase Splitting of Pyrene-Tetralin Mixtures," In Press *FUEL* (1988).

Shinnar, R.J., "On the Behavior of Liquid Dispersions in Mixing Vessels," *J. Fluid Mech.,* **10,** 259 (1961).

Shinnar, R.J. and J.M. Church, "Statistical Theories of Turbulence in Predicting Particle Size in Agitated Dispersions," *Ind. Eng. Chem.,* **52,** 253 (1960).

Sriram, K. and R. Mann, "Dynamics Gas Disengagement: A New Technique for Assesing the Behavior of Bubble Columns," *Chem. Eng. Sci.,* **32,** 571 (1977).

Stamatoudis, M. and L.L. Tavlarides, "Effect of Continuous Phase Viscosity on the Drop Sizes of Liquid-Liquid Dispersions in Agitated Vessels," *Ind. Eng. Chem. Process Des. Dev.,* **24,** 1175 (1985).

Taylor, G.I., "The Formation of Emulsion in Definable Fields of Flow," *Proc. Roy. Soc. Lond.* **A146,** 501 (1934).

Taylor, G.I., "Distribution of Velocity and Temperature between Concentric Rotating Cylinders," *Proc. Roy. Soc. Lond.* **A151,** 494 (1935).

Taylor, G.I., "The Spectrum of Turbulence," *Proc. Roy. Soc. Lond.* **A164,** 476 (1938).

Thomas, R.M., "Bubble Coalescence in Turbulent Flows," *Int. J. Multiphase Flow,* **7,** 709 (1981).

Todtenhaupt, E.K., "Blasengroβenverteilung in Techischen Begasung Sapparaten," *Chem. Ing. Tech.,* **43,** 336 (1971).

Tsuge, H. and S. Hibino, "Bubble Formation from a Submerged Single Orifice accompanied by Pressure Fluctuations in Gas Chamber," *J. Chem. Eng. Japan,* **11,** 173 (1978).

Tsuge, H. and S. Hibino, "Bubble Formation from an Orifice Submerged in Liquids," *Chem. Eng. Commun.,* **22,** 63 (1983).

Ueyama, K. and T. Miyauchi, "Properties of Recirculating Turbulent two Phase Flow in Gas Bubble Columns," *A.I.Ch.E. J.,* **25,** 258 (1979).

Vasalos, I.A., E.M. Bild, D.N. Rundell and D.F. Tatterson, "Experimental Techniques for Studing Fluid Dynamics of H-COAL Reactor," *Coal Processing Technology, CEP Technical Manual,* **6,** 226 (1980).

Weinstein, B. and R.E. Treybal, "Liquid-Liquid Contacting in Unbaffled Agitated Vessels," *A.I.Ch.E. J.,* **19,** 304 (1973).

Wraith, A.E., "Two Stage Bubble Growth at a Submerged Plate Orifice," *Chem. Eng. Sci.,* **26,** 1659 (1971).

Ying, D.H., E.N. Givens and R.F. Weimer, "Gas Holdup in Gas-Liquid and Gas-Liquid-Solid Flow Reactors," *Ind. Eng. Chem. Process Des. Dev.,* **19,** 635 (1980).

Yoshida, F. and T. Yamada, "Average Size of Oil Drops in Hydrocarbon Fermentors," *J. Ferment. Technol.,* **49,** 235 (1971).

Zakrzewski, W., J. Lippert, A. Lubbert and K. Schugerl, "Charakterisierung von Blasensaulen Durch Turbulenzmessungen," *Chem. Ing. Tech.*, **53,** 135 (1981).

APPENDICES

APPENDIX A

Calculation of the Energy Dissipation Rate in Tubular Reactors

The energy balance between the bottom and the top of the reactor can be used to determine the energy dissipation rate. The energy at the bottom includes the kinetic, potential and surface energy of bubbles. The energy at the top includes the kinetic and surface energy of bubbles. If it is assumed that the bubbles do not break up or coalesce while passing through the reactor, then the change in surface energy can be taken as zero. The velocity of bubbles also does not change significantly during the passage through the reactor, this indicates that the change in kinetic energy is negligible. Hence, the energy dissipated in the reactor with an initial height of H_0 cm is as follows:

$$\Delta E = E_{bottom} - E_{top}$$

where

$$E_{bottom} = 1/2\ \ mu_1^2 + \Delta\rho\ g\ H\ Q\ ,$$

$$E_{top} = 1/2\ \ mu_1^2\ ,$$

m is the mass flow rate of gas and Q is the volumetric flow rate of gas. Taking into account the above stated assumptions,

$$\Delta E = \Delta\rho\ g\ H\ Q$$

The energy dissipation rate per unit mass of liquid becomes:

$$\varepsilon = \frac{\Delta\rho \, g \, H \, u_g}{\rho_l \, H_o} \qquad \text{(A.1)}$$

Where $\Delta\rho$ is the density difference between the continuous phase liquid and gas, ρ_l is the density of the continuous phase liquid and H is the head pressure in cm of liquid in the reactor.

APPENDIX B

Maximum Drop Size against Break-up at Low Gas Fluxes

When a bubble is rising independently in a low viscosity liquid, a boundary layer is formed around its surface. The equations governing the boundary layer have been studied by Moore (1962,1965). It has been shown that the thickness of the boundary layer is proportional to $d_e Re^{-0.5}$, where d_e is the equivalent diameter of the bubble and Re is the Reynolds number. It has also been shown that the velocity changes within the order of magnitude of the terminal velocity of the bubble. In a flow field where bubbles are rising independently, drops follow the streamlines. Head-on collisions are not excluded but the probability of such events is very small. Moore (1965) also argued that the shear stresses are concentrated around the equator of bubbles. A drop in such a shear field tends to rotate, accelerate and deform. If the velocity gradients are large enough and interfacial tension forces are no longer able to maintain the drops intact they rupture. Taking into consideration all the above statements, the shear rate is of the order:

$$G \sim \frac{U_T}{d_e Re^{-0.5}} \qquad \text{(B.1)}$$

Substituting $Re = U_T d_e \rho_l / \mu_c$ into Equation B.1 and combining it with the Equation 2.2, Equation B.1 may be rewritten as:

$$G \sim \frac{U_T^{0.5}}{(\nu/g)^{0.5}} \qquad \text{(B.2)}$$

Taylor (1934) argued that a drop of size d_p in a simple shear field will break up if the ratio of viscous forces over interfacial tension forces exceeds unity. Therefore, a criterion for break-up is:

$$G\mu_c f(p) > \sigma/d_p \qquad \text{(B.3)}$$

where G is the shear rate taken from Equation B.2, f(p) a function accounting for the relative viscosity and p is the relative viscosity, μ_d/μ_c. After some manipulation Equation B.3 may be expressed as:

$$d_{max} \sim \frac{\sigma}{(\mu_c \rho_l g)^{0.5} f(p) U_T^{0.5}} \qquad \text{(B.4)}$$

At low gas fluxes $U_T \alpha u_g$ (see APPENDIX D). Therefore, Equation B.4 can be rewritten as:

$$d_{max} \alpha \frac{\sigma}{(\mu_c \rho_l g)^{0.5} f(p) u_g^{0.5}} \qquad \text{(B.5)}$$

Equation B.4 gives the order of magnitude of maximum stable drop size against break-up in tubular reactors at low gas fluxes. Equation B.5 includes the qualitative information that d_{max} is expected to change as a function of $u_g^{-0.5}$.

APPENDIX C

Minimum Drop Size against Coalescence at Low Gas Fluxes

The mechanism of coalescence includes the two following stages:

- The draining of the intervening film of continuous phase liquid to a critical thickness h.
- The rupture of the remaining film by a mechanism not completely understood.

It will be supposed that the two drops are pressed together by a steady force F, which is related to viscous forces and that drainage takes place between rigid planes. Calculation of the time τ required for the film to drain to the thickness h is a classical lubrication problem and the solution is given by Thomas (1981) as:

$$\tau = \frac{3\pi\mu_c s^4}{2Fh^2} \qquad (C.1)$$

where s is the radius of the film, μ_c the viscosity of the continuous phase liquid and F is the force pressing the drops together. Considering the pressure within the drop gives:

$$F=4\pi s^2\sigma/d_p \qquad (C.2)$$

so the film-drainage time may be rewritten as:

$$\tau = \frac{3}{32\pi} \mu_c F(d_p/\sigma h)^2 \qquad (C.3)$$

The viscous forces may be expressed as:

$$F=\pi d_p^2 \mu_c G f(p) \qquad (C.4)$$

Combining Equations C.2, C.3 and C.4, Equation C.4 can be expressed as:

$$\tau= \frac{3}{32\pi} \mu_c \pi d_p^2 G f(p)(d/\sigma h)^2 \qquad (C.5)$$

If one denotes by T the characteristic timescale of a two-drop encounter and assuming that viscous forces are the cause of drop movement, dimensional analysis yields:

$$T \sim d_p/U_T$$

where d_p is the diameter of drop and U_T is the terminal velocity of bubble. A simple criterion for coalescence is $\tau < T$, which gives after some manipulation:

$$d_{man} \sim 2.2\ U_T^{-0.5}\ f(p)^{-1/3}(\sigma h/\mu_c)^{2/3}(\nu/g)^{1/6} \qquad (C.6)$$

At low gas fluxes $U_T \sim u_g$ (see APPENDIX D). Therefore, Equation C.6 may be rewritten as:

$$d_{min} \alpha\ u_g^{-0.5}\ f(p)^{-1/3}(\sigma h/\mu_c)^{2/3}(\nu/g)^{1/6} \qquad (C.7)$$

Equation C.6 gives the order of magnitude of minimum stable drop size against coalescence in tubular reactors at low gas fluxes. Equation C.7 includes the qualitative information that drop size is expected to change as a function of $u_g^{-0.5}$.

APPENDIX D

Relationship Between Superficial Gas Velocity and Terminal Velocity of Bubbles at Low Gas Fluxes

Suppose that at an instant in the tubular reactor the superficial gas velocity is u_g, the number of bubbles per unit of time N and that the bubbles are of uniform diameter d_b and volume V_b. If the superficial velocity increases to u_g+du_g, where du_g represents an infinitesimal increment, then the number of bubbles per unit of time will be N+dN of diameter d_b+dd_b and volume V_b+dV_b. Writing down a mass balance for the gas and considering constant density, one gets:

$$Adu_g=NdV_b+dN(V_b+dV_b) \qquad (D.1)$$

where A is the cross-section area. Cancelling out the term $dNdV_b$ and integrating using $u_g=0$ when N=0, Equation D.1 may be rewritten as:

$$u_g=NV_b/A \qquad (D.2)$$

Now if one considers a swarm of bubbles covering completely the volume of the reactor, then the probability including both events for a head-on collision between a drop and bubble and a drop being trapped in the boundary layer of a bubble, is unity.

$$p=1 \quad \text{and} \quad N'=V/V_b \qquad (D.3)$$

where p represents probability, N' number of bubbles and V the volume of the

tubular reactor. When N bubbles are present in the reactor, then the probability becomes:

$$p=N/N' \quad \text{or} \quad p=NV_b/V \tag{D.4}$$

If the superficial gas velocity u_g increases, the number of bubbles will increase to N+dN and their volume to V_b+dV_b. Then the probability will be:

$$p+dp=(N+dN)/N' \tag{D.5}$$

Using Equations D.3, D.4 and D.5 and integrating using that p=0 when N=0, one gets:

$$p=NV_b/V \tag{D.6}$$

Combining Equations D.5 and D.6 one ends up with:

$$p \propto u_g \tag{D.7}$$

Now consider that the number of drops per unit volume of the reactor is η and a bubble moving indepedently with its terminal velocity U_T. Within a fixed time t this bubble will travel a distance $l_1=U_Tt$ and have a probability p to collide with a drop or to entrap a drop in its boundary layer. For another bubble moving with velocity U_T+dU_T, the covered distance during the same time will be $l_2=(U_T+dU_T)t$ and the probability p+dp. If one considers a uniform distribution of drops in the reactor, then:

$$l_1/l_2=\eta_1/\eta_2=p/(p+dp)=U_T/(U_T+dU_T) \tag{D.8}$$

Integrating Equation D.8, one may write:

$$p \propto U_T \qquad (D.9)$$

Combining Equations D.7 and D.9, the following relationship can be obtained:

$$u_g \propto U_T \qquad (D.10)$$

From a statistical point of view, Equation D.10 holds reasonably well. Sriram (1977) has defined the superficial gas velocity given in section 2.3 as Equation 2.7. If consideration of uniform bubble size is employed, then Equation D.11 may be obtained:

$$u_g = \varepsilon_g U_T \qquad (D.11)$$

Since gas hold-up does not change much and may be considered almost constant for superficial velocities in the range (0.1-0.3 cm/sec), the superficial gas velocity u_g can be considered as proportional to terminal velocity of uniform size bubble U_T.